Supramolecular Behaviour of Meldrum's Acid-Based Ligand with Cucurbit[*n*]urils

Supramolekulární chování ligandu na bázi Meldrumovy kyseliny s cucurbit[n]urily

Bc. Vít Guiglielmo Mišurec

Master's thesis
2023

Tomas Bata University in Zlín
Faculty of Technology

Univerzita Tomáše Bati ve Zlíně
Fakulta technologická
Ústav chemie

Akademický rok: 2022/2023

ZADÁNÍ DIPLOMOVÉ PRÁCE

(projektu, uměleckého díla, uměleckého výkonu)

Jméno a příjmení:	**Bc. Vít Guiglielmo Mišurec**
Osobní číslo:	**T21451**
Studijní program:	**N0721A210005 Chemie potravin a bioaktivních látek**
Forma studia:	**Prezenční**
Téma práce:	**Supramolekulární chování ligandu na bázi Meldrumovy kyseliny s cucurbit[n]urily**

Zásady pro vypracování

I. Teoretická část

- Supramolekulární chemie a fotochemie
- Syntéza, fyzikálně-chemické vlastnosti a aplikace donorně-akceptorních Stenhousových aduktů

II. Praktická část

- pomocí dostupných metod (ITC, MS, NMR) prozkoumat supramolekulární chování ligandu na bázi Meldrumovy kyseliny s vybranými homology CBn

Forma zpracování diplomové práce: **tištěná/elektronická**

Seznam doporučené literatury:

1. B. L. Feringa et al.: The (photo)chemistry of Stenhouse photoswitches:guiding principles and system design. Chem. Soc. Rev. 2018, 47, 1910-1937.
2. B. L. Feringa et al.: Unraveling the Photoswitching Mechanism in Donor-Acceptor Stenhouse Adducts. J. Am. Chem. Soc. 2016, 138, 6344 – 6347.
3. B. D. Wagner et al.: Photophysical Properties of Donor-Acceptor Stenhouse Adducts and Their Inclusion Complexes with Cyclodextrin and Cucurbit[7]uril. Molecules 2020, 25, 4928.

Vedoucí diplomové práce: **doc. Ing. Michal Rouchal, Ph.D.**
Ústav chemie

Datum zadání diplomové práce: **31. prosince 2022**
Termín odevzdání diplomové práce: **12. května 2023**

L.S.

prof. Ing. Roman Čermák, Ph.D.
děkan

doc. Ing. Michal Rouchal, Ph.D.
ředitel ústavu

Ve Zlíně dne 28. února 2023

THESIS AUTHOR STATEMENT

Beru na vědomí, že:

- diplomová práce bude uložena v elektronické podobě v univerzitním informačním systému dostupná k prezenčnímu nahlédnutí;
- na moji diplomovou práci se plně vztahuje zákon č. 121/2000 Sb. o právu autorském, o právech souvisejících s právem autorským a o změně některých zákonů (autorský zákon) ve znění pozdějších právních předpisů, zejm. § 35 odst. 3;
- podle § 60 odst. 1 autorského zákona má Univerzita Tomáše Bati ve Zlíně právo na uzavření licenční smlouvy o užití školního díla v rozsahu § 12 odst. 4 autorského zákona;
- podle § 60 odst. 2 a 3 autorského zákona mohu užít své dílo – diplomovou práci nebo poskytnout licenci k jejímu využití jen s předchozím písemným souhlasem Univerzity Tomáše Bati ve Zlíně, která je oprávněna v takovém případě ode mne požadovat přiměřený příspěvek na úhradu nákladů, které byly Univerzitou Tomáše Bati ve Zlíně na vytvoření díla vynaloženy (až do jejich skutečné výše);
- pokud bylo k vypracování diplomové práce využito softwaru poskytnutého Univerzitou Tomáše Bati ve Zlíně nebo jinými subjekty pouze ke studijním a výzkumným účelům (tj. k nekomerčnímu využití), nelze výsledky diplomové práce využít ke komerčním účelům;
- pokud je výstupem diplomové práce jakýkoliv softwarový produkt, považují se za součást práce rovněž i zdrojové kódy, popř. soubory, ze kterých se projekt skládá. Neodevzdání této součásti může být důvodem k neobhájení práce.

Prohlašuji,

- že jsem na diplomové práci pracoval samostatně a použitou literaturu jsem citoval. V případě publikace výsledků budu uveden jako spoluautor.
- že odevzdaná verze diplomové práce a verze elektronická nahraná do IS/STAG jsou obsahově totožné.

Ve Zlíně, dne:

Jméno a příjmení studenta:

. . . . . .

podpis studenta

Abstrakt

Tato práce zkoumá chování donorně-akceptorových Stenhousových aduktů (DASA) syntetizovaných z Meltrumovy kyseliny a interakce s cucurbit[n]urily v kapalné a plynné fázi. Analyzované sloučeniny patrí do 1. generace nedávno objevených fotospínačů, jejichž kvality monou být využity ve velké škále vědeckých oborů včetně supramolekulární chemie. Analýzy byly provedeny pomocí hmotnostní spektrometrie (ESI-IT-MS), nukleární magnetické rezonance a UV-Vis spektrofotometrie. Výzkum úspěšně popisuje tvorbu komplexů s cucurbit[7]urilem pomocí NMR a UV-Vis analýzou a základní chování DASA v plynné fázi. Navíc byla hrubě stanovena vazebná konstanta komplexu otevřené formy DASA s cucurbit[7]urilem. Využití DASA v supramolekulárních komplexech je zajímavou cestou jak propojit supramolekulární chemii a fotochemii s vysokým potenciálem.

Klíčová slova: Donorně–akceptorní Stenhousovy adukty, cucurbit[n]urily, chemie systémů hostitel–host, hmotnostní spektrometrie, nukleární magnetická rezonance, UV-Vis spektrometrie.

Abstract

This thesis examines the behaviour of a donor-acceptor Stenhouse adduct (DASA) synthesised from Meldrum's acid and the interaction with cucurbit[n]urils in the liquid and gas phase. The analysed compound belongs to the 1st generation of recently discovered photoswitches, whose qualities could be used in a vast range of fields of science, including supramolecular chemistry. The analyses were performed by mass spectrometry (ESI-IT-MS), nuclear magnetic resonance, and UV-Vis spectrophotometry. The research successfully describes the formation of a complex with cucurbit[7]uril by NMR and UV-Vis analysis and the elementary behaviour of

the DASA in the gas phase. Additionally, the binding constant of the complex of the open form of DASA with cucurbit[7]uril was estimated. Using DASA in a supramolecular complex is an interesting way to combine supramolecular chemistry and photochemistry with a great potential.

Keywords: Donor–acceptor Stenhouse adducts, cucurbit[n]urils, host–guest chemistry, mass spectrometry, nuclear magnetic resonance, UV-Vis spectrometry.

First of all, I would like to express my deepest gratitude to doc. Ing. Michal Rouchal, Ph.D. for his relentless support and immense efforts without which this thesis would not have come into being. I would also like to deeply thank Prof. Dr. Uwe Pischel for his valuable advice, groundbreaking research in this field and the materials he graciously provided.

This thesis would not have been successful either without the help of Ing. Aneta Závodná, who was always ready to discuss and consult throughout the whole process of the research. And last but not least I would like to thank Ing. Petr Janovský for his brilliant mathematical models and predictions which greatly helped in designing the experiments.

Aside from the academic contributions, great thanks go to my dearest and wisest wife, for her patient and detailed linguistic and stylistic corrections and advice throughout writing the thesis.

TABLE OF CONTENTS

INTRODUCTION

Chemical compounds controllable remotely by a non-destructive method are a point of interest for a lot of research groups. One category of these compouds are those controllable by light - photoswitches. One group of the new, emerging photoswitches are the donor-acceptor Stenhouse adducts, DASAs for short. DASAs were first mentioned in 2014, since then 3 generations of them have been designed. The upgrades between the generations are focused on the tunability of the switches. After nine years there are still lot of blank spaces to fill even in case of the 1st generation. This thesis will attempt to fill a few of these gaps. The experiments of this thesis are part of a vaster research about DASAs within the research groups of Prof. Dr. Uwe Pischel, University of Huelva, and Robert Vícha, Tomas Bata University in Zlín. Researching a new compound or group is always full of challenges and surprises, neither of which were missing in our experiments.

DASAs' behaviour is strongly affected by the environment: depending on the type of the solvent DASAs tend to be open (linear), closed (cyclic), or to switch between the forms depending on light. In protic solvents, therefore also in biological systems, DASAs tend to close. This phenomenon was already researched for biological applications. An example could be designing derivatives of DASA with ambiphilic properties in open form, which can be lost by closing it using light enabling the micelles assembled of the derivatives to be dissolved on command. The idea of transporting DASA to a certain spot and then releasing or activating it in another way by light could be applied to supramolecular systems. The host–guest interactions of DASAs with macrocycles are one of the main topics of this thesis, specifically the interactions with cucurbit[n]urils. The experiments with cucurbit[n]urils represent the main challenge in this research. The reason is supramolecular experiments with cucurbit[n]urils are performed in an aqueous environment, in which the open form of DASA, which is able to enter inside the cavity of cucurbit[n]urils, is gradually closed. One of the aims of this research is also to find a solution for this paradox.

The element of surprise is provided by the analysis of DASA in gas phase, which is a completely unresearched area of DASA. From the innovativeness of the experiments it

is clear, that they will either lay a foundation for further, more detailed research or the results will clearly show, that the direction is wrong.

I. THEORETICAL PART

1 Supramolecular chemistry

Like every branch of science, supramolecular chemistry does not have a precise definition either. Originally, supramolecular chemistry was defined as a field dealing with non-covalent interactions between a 'host' and a 'guest' molecule. [1] At first sight, it seems like a perfect and easy definition, but these descriptions are by their nature noncomprehensive and can cause misunderstandings if taken too literally. The modern approach embraces not just the host–guest systems but also molecular machines and devices, [2] molecular recognition, [3] self-organisation or self-assembly. [4] Therefore, a more suitable definition is the one proposed by Jean-Marie Lehn, who describes supramolecular chemistry as the 'chemistry of molecular assemblies and of the intermolecular bond'. For the host–guest chemistry it is necessary to define how the given complex is formed. A complex is generally produced by a 'host' molecule binding to an another, 'guest' molecule. Commonly, the host is a large molecule (eg an enzyme or a macrocycle) weighing up to several thousand daltons, while the guest may range from a monoatomic cation/anion to sophisticated molecules such as hormones or drugs. The host–guest complex is not necessarily composed of one host and one guest, it can comprise multiple molecules including different types of hosts or guests. The host–guest complexes are primarily defined by their stoichiometry as well as binding constant, geometry, and energy.

1.1 Binding constant and binding energy

The binding constant K is a dimensionless quantity expressing the thermodynamic stability of a host–guest complex depending on the solvent and temperature, although it is often expressed as the equilibrium constant for the reaction shown in equation (1.1) between a guest (G) and a host (H), which creates the supramolecular complex G@H. [1]

$$a\,\mathrm{G} + b\,\mathrm{H} \underset{k'}{\overset{k}{\rightleftharpoons}} \mathrm{G@H} \tag{1.1}$$

The coefficients a and b represent stoichiometric coefficients. As mentioned before, the binding constant is strictly dimensionless, but when calculated approximately using concentrations, units are assigned to the constant depending on the stoichiometry of the complex, eg for a 1:1 complex the units are $\mathrm{dm^3 \cdot mol^{-1}}$ or $\mathrm{M^{-1}}$. For the equation

on (1.1), the binding constant is expressed as:

$$K = \frac{[\mathrm{G@H}]}{[\mathrm{G}]^a\,[\mathrm{H}]^b} \tag{1.2}$$

The binding constant may also be defined by the rate constants k of the association and dissociation of the complex:

$$K = \frac{k}{k'} \tag{1.3}$$

Despite the importance of the binding constant, the selectivity of some supramolecular systems has been reported to be heavily influenced by temperature, therefore thermodynamic parameters are more suitable criteria for expressing molecular recognition abilities. Enthalpy ΔH, entropy ΔS and Gibbs free energy ΔG are linked to the binding coefficient in (1.4) and through (1.5) in (1.6).

$$\Delta G = -RT \ln K \tag{1.4}$$

$$\Delta G = \Delta H - T\Delta S \tag{1.5}$$

$$\ln K = -\frac{\Delta H}{R} \cdot \frac{1}{T} + \frac{\Delta S}{R} \tag{1.6}$$

1.2 Cucurbit[n]urils and other common hosts

In supramolecular chemistry one of the relatively new families of host molecules is represented by cucurbit[n]urils (CB[n]). The first of its kind, CB[6], was firstly descibed in 1981 [5] and its use in supramolecular chemistry was researched throughout the 1980s and 1990s. [6] Upon further research other homologues were discovered, most importantly CB[5]–CB[8], and CB[10]. The new family of macrocycles found use in a wide range of applications such as chromatographic stationary phase, the sequestration of contaminants from solutions, [7] and the development of catalysts, [8] chemical sensors, [9] and new drugs. [8] From the structural side, cucurbiturils are cyclic methylene-bridged glycoluril oligomers. The structure of CB[n]s (the CB[7] and CB[8] homologues are depicted on Fig. 1) resembles a pumpkin, which is where the name comes from (*cucurbitaceae* in latin). Cucurbiturils present a competition for other hosts, including the traditional group, cyclodextrins. Cyclodextrins are cyclic oligosaccharides consisting of D-glucopyranoside units linked via an α-1,4-glycosidic bond. [10] On one hand, CB[n]s are limited by their relatively poor solubility in water: CB[5] and CB[7] are mildly

soluble, whereas CB[6] and CB[8] are essentially insoluble, although the solubility can be dramatically improved in concentrated aqueous acids. On the other hand, the key advantage of CB[n]s is their high thermal stability: all CB[n]s are capable of resisting up to 370 °C. [6] Physical and other properties of CB[n]s in comparison with cyclodextrins are presented in Tab. 1.

Tab. 1: Dimensions and physical properties of cucurbit[n]urils and cyclodextrins. [6]

	M_r	a [Å]	b [Å]	c [Å]	V [Å^3]	s_w [mM]	Stability [°C]
CB[5]	830	2.4	4.4	9.1	82	20–30	> 420
CB[6]	996	3.9	5.8	9.1	164	0.018	425
CB[7]	1163	5.4	7.3	9.1	279	20–30	370
CB[8]	1329	6.9	8.8	9.1	479	< 0.01	> 420
α-CD	972	4.7	5.3	7.9	174	149	297
β-CD	1135	6.0	6.5	7.9	262	16	314
γ-CD	1297	7.5	8.3	7.9	427	178	293

M_r relative molar mass; a, b, c van der Waals radii of a macrocycle (Fig. 1); V volume; s_w solubility in water.

Besides cucurbiturils and cyclodextrins, other commonly used hosts are calix[n]arenes [11] and pillar[n]arenes, [12] bambusurils, [13] crown ethers, [14] cyclophanes etc. [15] Through the years macrocycles related to cucurbiturils were discovered, too, such as

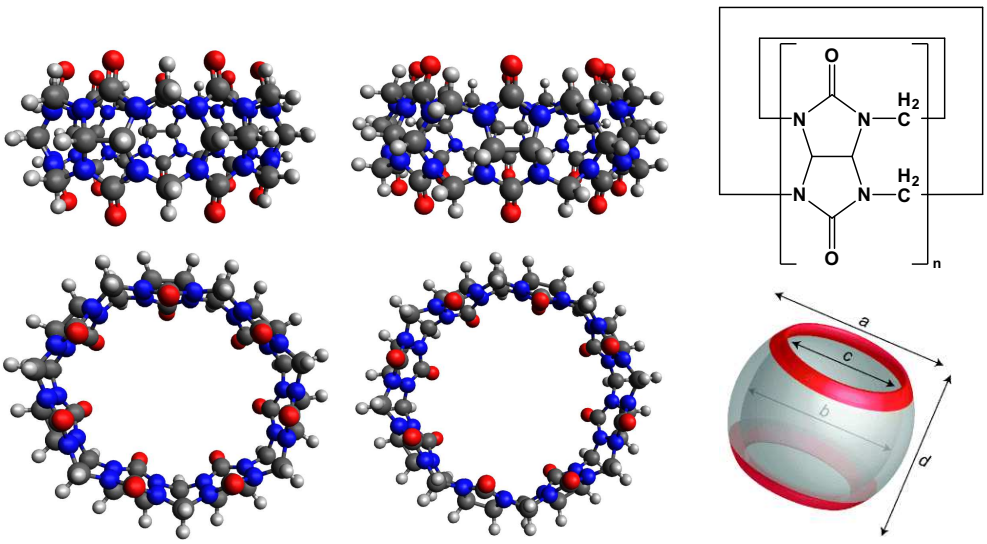

CB[7] CB[8]

Fig. 1: Chemical structure of cucurbit[n]urils (CB[n], $n = 5 - 8$), X-ray structures of CB[7] and CB[8], and depiction of the van der Waals radii. [6]

hemicucurbiturils, [16] substituted cucurbiturils, *nor-seco*-cucurbiturils or (±)-bis-*ns*-cucurbiturils. [15] The main difference between them lies in their guest–binding affinity and dissociation rates.

1.3 Supramolecular photochemistry

A prospective field of research is the combination of supramolecular chemistry and photochemistry. This field combines the study of a multitude of various abilities of assembly and deassembly of the host–guest or macromolecular systems, photoisomerisation and related photoswitching, photosynthesis, photopolymerisation, etc. To demonstrate the possibilities of supramolecular chemistry, a few examples using the macrocycles or photosensitive compounds studied in this thesis will be presented. The cucurbit[*n*]urils, due to their dimensions and internal environment, became an object of interest in the field of photodimerisation. The use of cucurbiturils for the dimerisation of eg derivatives of coumarin, cinnamic acid, or azostilbenes has been investigated for years. [17] By designing the moieties of the derivatives it is possible to affect which adduct will prevail. Another great example from the host–guest photochemistry is increasing the binding constant by light. Diaminostilbenes switch between the *Z* and *E* isomer in standard conditions. [18] *E*-diaminostilbene in complex with CB[7] can undergo the photoisomerisation inside the cavity into *Z*-diaminostilbene. The reverse isomerisation does not occur spontaneously inside the CB[7] and thus the binding constant becomes three times higher.

The derivatives from photoswitches such as diazobenzene of donor–acceptor Stenhouse adducts (DASA, *vide infra*) can be operated by light in order to control large dynamic supramolecular systems. [19] Open isomers are capable of creating micels, nanofibres or macroscopic scaffolds, which deassemble after irradiation (due to the photoisomerisation of DASA) and either release a drug or reassemble into different constructs, eg vesicles.

Supramolecular photochemistry has a potential not only in medicine and bioapplications, but also in industry as a sensors, [20] molecular machines, [21] logic gates, [22] or solar energy convertors. [23] Light induced technologies have higher

chances to be accepted by society, both by progressives and conservatives, as they are driven by a 'green' and familiar power.

1.4 Supramolecular chemistry in the field of bioactive compounds

Supramolecular complexes are based on the mechanism of self-assembly. In the field of bioactive compounds, it is possible to see the mechanism from two points of view: i) either self-assembled complexes are implanted into the organism and deassemble after reaching the destined tissue, or ii) a defined mixture of compounds is implanted and after reaching the specific medium the molecules self-assemble into an effective complex. Both methods could be useful and very promising for the future of drugs and treatment of various diseases.

In case of the first method, cucurbiturils and cyclodextrins are vastly used. These cavitands are amphiphilic with a hydrophobic interior and a hydrophilic exterior in aqueous solutions. [10] The capability of cyclodextrins of forming complexes with larger hydrophobic guests led to multiple applications in drug delivery, due to their ability to enhance certain properties of drugs, such as solubility, [24] stability (primarily in aqueous solutions), [25] bioactivity, [26] bioavailability for most applications (eg oral, [27] buccal, [28] nasal, rectal, [29] vaginal, [30] transdermal, or ocular), and drug distribution through time by slowing or delaying the drug impact. [31] A vaster range of binding constants of cucurbiturils introduces an element of switchability to host–guest-based systems, when a bound guest is displaced by a higher affinity guest. [10] This capability improves the targetability of the drug distribution: the encapsuled drug can be released not only by light excitation, a change in pH or by redox potential, [32] but also by a competitive guest, which can appear only in an exact spot of the organism and thus enabling the drug to be released only exactly where it is needed. Cucurbiturils are also capable of forming a ternary complex with two guests molecules (with the same or different structure). [33] Such a versatile mechanism can be used to build immensely sophisticated complexes, such as nanozymes. [34]

In case of the second method, popular macromolecular chains are used to build the supramolecular complexes. The self-assembling complexes have high potential in multiple disciplines. Regarding bioactive compounds the most promising aspect is a new generation of drugs. [15] The potential of supramolecular nanomedicines lies in the aspects below. The technology allows us to use compounds that have been

already researched extensively, meaning that their potential side effects in case of human use are already well known, thus drugs can be designed using compounds with minimal or even no side effects. [35] Additionally, the technology enables us to design self-assembling drug in a way that the assembly occurs only in the target site, triggered by, for example, a unique pH or an excess of enzymes. Probably the biggest advantage of self-assembling drugs over macrocycles is an easier transport through biological barriers, including the most challenging blood-brain barrier. [36]

Even though the two methods are placed in contrast, the line between them is very thin; in lot of cases both methods are researched and have a high potential for the future of drugs and treatments of illnesses untreatable at present.

2 Photochemistry

All chemical transformations are affected by the activation energy. Some of them do not need a high amount of energy and can occur in laboratory conditions, while others need such intense energy, that heat only cannot trigger the reaction. Energy is delivered in two forms – heat and light – serving as a basis for the division of the field to thermochemistry and photochemistry, respectively. [37]

Light exhibits the behaviour of both waves and particles. Wave theory explains some characteristics of light perfectly, like reflection or polarisation, whereas, eg the photoelectric effect can be explained only if light is interpreted as a beam of particles. The processes occurring in photochemical reactions are described by quantum physics. [38] The energy of each photon E_{ph} in a light beam with a specific frequency ν is determined as

$$E_{ph} = h\nu = \frac{hc}{\lambda} \tag{2.1}$$

where λ is the wavelength, c the speed of light and h is Planck constant. Considerable energy levels range from 126 to 586 kJ·mol^{-1}, which corresponds to wavelengths in the interval from ca 950 to 205 nm, which covers the whole visible spectrum (VIS, $\lambda \in [400; 750]$ nm) as well as a significant part of the ultraviolet (UV, $\lambda \in [10; 400]$ nm) and the near-infrared spectra (NIR, $\lambda \in [750; 1500]$ nm). To compare excitation by light and heat, if energy of 126 kJ is added to a mole of water, its temperature rises by more than 2000 K. These temperature levels would destroy most molecular samples.

2.1 Photochemical and photophysical processes

Before listing and explaining the individual processes, the difference between photochemistry and photophysics will be summarised. [37] As long as the consequence of excitation does not induce changes in the chemical structure or configuration of the molecule, the process is photophysical. Contrarily, in the photochemical processes the initial and terminal molecules are not identical.

The excitation of molecule A is usually indicated as

$$\mathrm{A} + h\nu \longrightarrow \mathrm{A}^* \tag{2.2}$$

To indicate an electronically excited species, the star index is used. Energy gained from a photon excites an electron to a higher vibrational state (marked with thin lines on

Fig. 2) of electronic state on which the electron can be energetically conserved (in isolated molecules). [39] Through vibrational relaxation (**vr**) the electron loses energy to the environment and reaches the lowest vibrational and rotational levels. Electronic levels are named after their spin multiplicity. The most important spin manifolds for even electron molecules are singlets (S_n) and triplets (T_n).

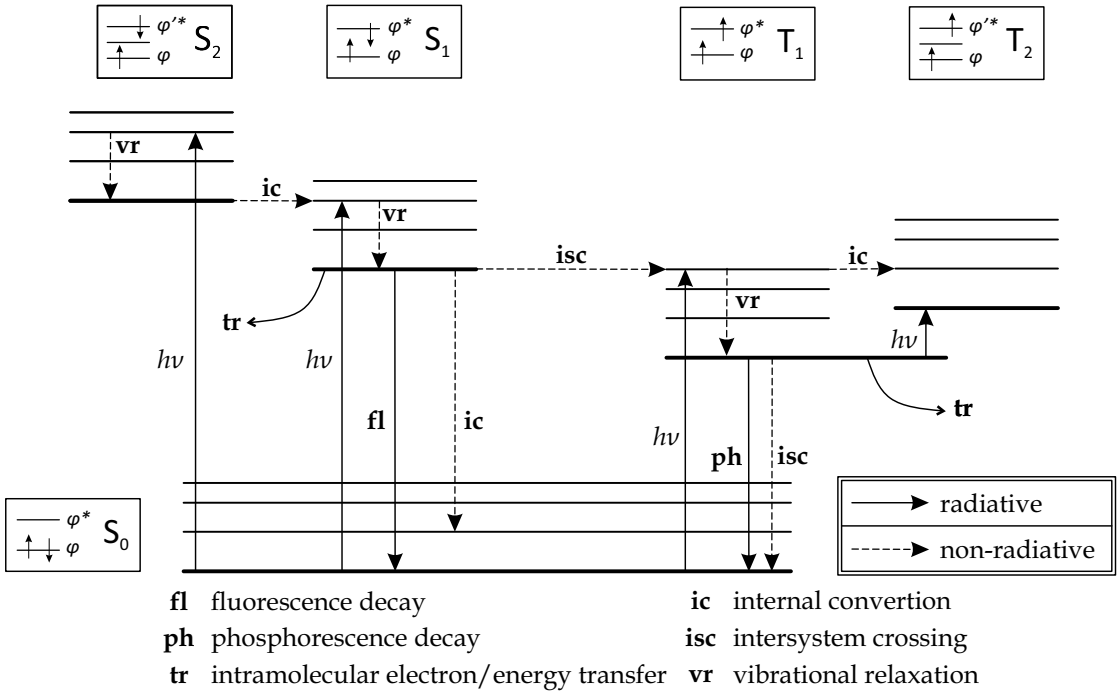

Fig. 2: Jabloński diagram (adapted from [37, 38, 39]).

The processes which link different vibrational or rotational levels on Fig. 2 are photophysical radiative or radiationless transitions, and as the diagram shows, the molecules are promoted from one state to another. [39] As mentioned, in photophysical processes no structural changes occur, although in different electronic states the bond lengths and angles vary. Radiative transitions, unlike radiationless ones, are associated with the absorption and emission of a photon. Besides the excitation of the molecule by light, other radiative transitions are fluorescence (**fl**) and phosphorescence (**ph**). In both cases of luminescence a photon is emitted, but **fl** is significantly quicker than **ph**. This is caused by the typical initial state (for **fl** it is typically a singlet, and for **ph** a triplet) and by spin change, which occurs during **ph** but not in **fl**. A radiationless transition (or decay) occurring between two electronic states of the same multiplicity is called an internal conversion (**ic**), and a transition between states of different multiplicity is known as intersystem crossing (**isc**).

Photochemical processes are various, an overview of the most common ones together with photophysical processes is displayed in Tab. 2.

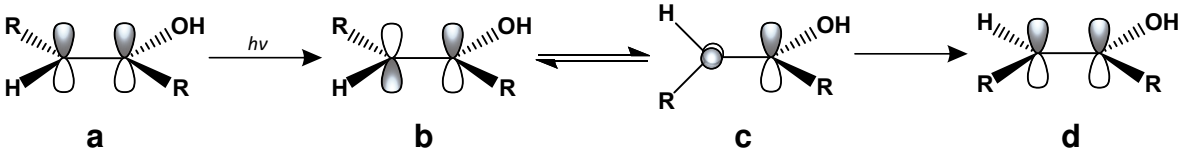

Fig. 3: Scheme of photoisomerisation: a Z isomer in a ground state **a** is illuminated causing an excitation of an electron and dissociation of a π–bond, [40] **b** with antibonding orbitals capable of freely rotating around the single C—C bond and switching through **c** into a E isomer **d**. [37]

In the context of this thesis, the key process is photoisomerisation, when absorbed energy is used to change conformation on a multiple bond ($E \longleftrightarrow Z$). The mechanism of photoisomerisation is based on the dissociation of a π–bond and the consequent rotation around the single C—C bond (see Fig. 3). [37] The process can be initiated both photochemically and thermally, resulting in different E/Z ratios. [38] In case of thermal induction, the ratio of Z and E isomers depends on their relative thermodynamic stabilities. In contrast, photoisomerisation of a double bond is governed by the ratio of the reciprocal quantum yields (Φ_{E-Z} and Φ_{Z-E}) and the molar absorption coefficients ε of the corresponding isomers:

$$\frac{[E]}{[Z]} = \frac{\varepsilon_Z^\lambda \Phi_{Z-E}}{\varepsilon_E^\lambda \Phi_{E-Z}} \tag{2.3}$$

Tab. 2: Overview of the common photochemical and photophysical processes [38]

Ionisation	$A^* \longrightarrow A^+ + e^-$	Normally requires high energies, an extremely fast process, the excess energy from ionisation converted into kinetic energy of the emitted electron.
Luminescence	$A^* \longrightarrow A + h\nu'$	Spontaneous emission of a photon of frequency ν', transition of the molecule to a lower state, usually $\nu' < \nu$.
Radiationless decay	$A^* \longrightarrow A$	No photon emission or chemical reaction, the energy converted into vibrational energy, includes internal conversion (**ic**) and intersystem crossing (**isc**)
Quenching	$A^* + B \longrightarrow A + B$	Transferring energy to the quencher B, after moving apart the excess energy transferred to the nuclear degrees of freedom.
Excitation transfer or sensitization	$A^* + B \longrightarrow A + B^*$	Similar to quenching, transferred energy high enough to excite B.
Photoisomerisation	$A^* \longrightarrow B$	A isomerises to B and reverts to the ground state by radiationless decay, photon energy used to overcome the activation barrier.
Photodissociation	$A^* \longrightarrow B + C$	The photon energy used to break a chemical bond, possibly producing two radicals.
Electron transfer	$A^* + B \longrightarrow A^+ + B^-$ $A^* + B \longrightarrow A^- + B^+$	An excited molecule becomes at once a better electron donor and electron acceptor.
Bimolecular reaction	$A^* + B \longrightarrow C + D$	Consists of many kinds of reactions, most of them based on the transfer of single or multiple atoms.
Addition reaction	$A^* + B + M \longrightarrow AB + M$	M does not react but withdraws part of the available energy from the otherwise unstable product AB.

3 Donor–acceptor Stenhouse adducts

3.1 General overview

The roots of donor–acceptor Stenhouse adducts (DASAs) reach back to the middle of the 19th century when John Stenhouse observed the behaviour of furfural in the presence of various organic substances. He discovered that furfural in combination with aniline changes its colour to pink–violet on different surfaces, such as paper, silk, linen canvas or cotton, but in equimolar aniline mixture he never succeeded to create coloured crystals. [41] Later, in 1870, Stenhouse returned to experimenting with furfuranilin with the aim of obtaining crimson crystals.

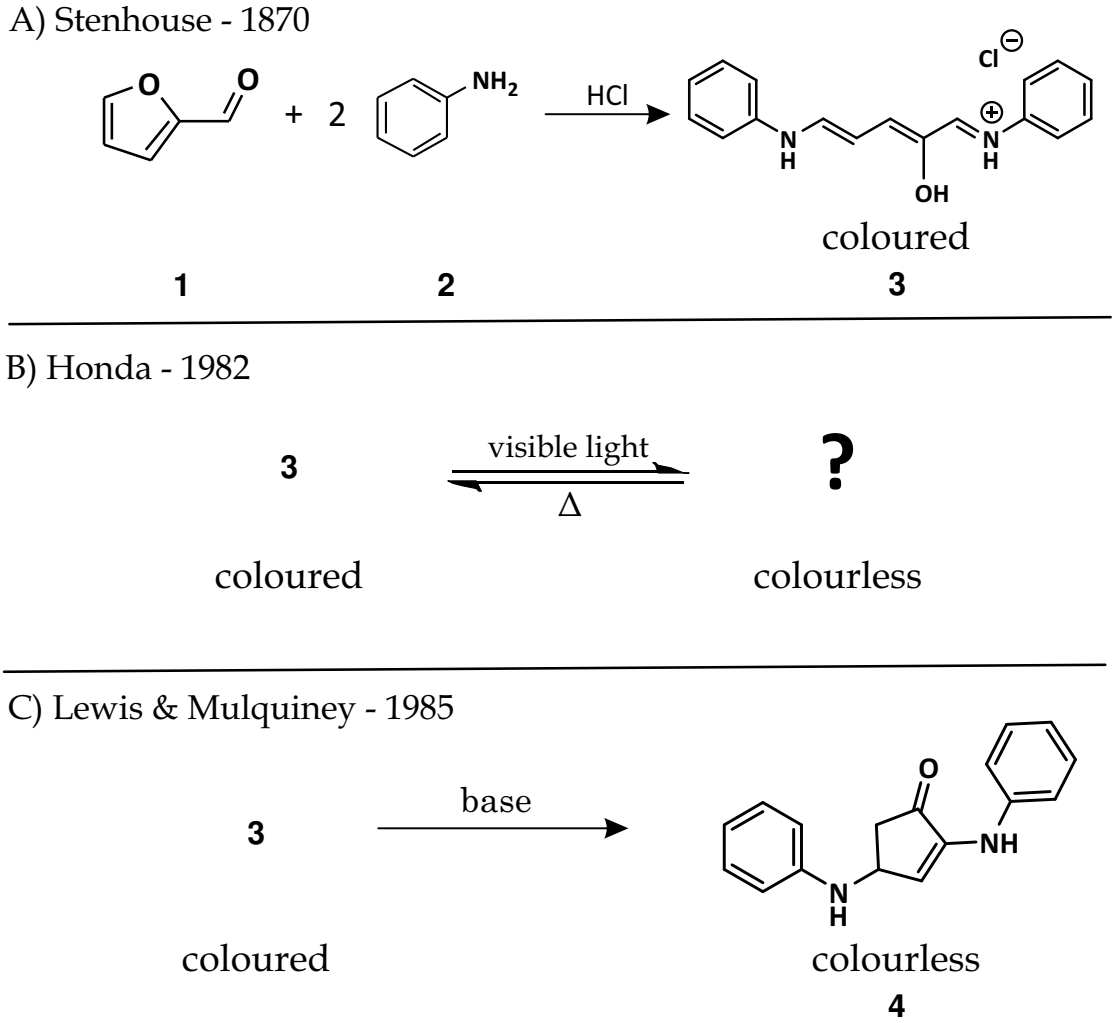

Fig. 4: Historical review of the evolution of Stenhouse salt (adapted from [42])

Stenhouse added aniline hydrochloride and ethanol to an equimolar solution of furfural (**1**) and aniline (**2**), and as a result of the reaction he attained the desired

crystals of **3** (Fig. 4A). Similar results were obtained also with nitric acid, but not with oxalic acid. [43] Schiff in his research confirms the properties and behaviour of furopolyamine salts and proves that similar results can be achieved with other primary monoamines (eg *m*-nitroaniline, *o*-toluidine, xylidine), secondary monoamines (eg *N*-methylaniline, *N*-ethylaniline, *N*-phenylaniline), diamines (eg phenylenediamine, 4,4'-diaminobiphenyl, urea) or aminoacids and their derivates (eg aminosalicylic acid, *p*-aminobenzoic acid, aminobenzamide). [44] Dissolved Stenhouse salts are unstable: the intensity of the colour of alcohol solutions changes negatively upon irradiation, while the colouring returns in the dark. The phenomenon was examined by Honda (Fig. 4B), [45] but the structural changes were specified by Lewis and Mulquiney three years later (Fig. 4C). [46] Based on the photochemical properties of Stenhouse salts, in 2014 DASAs – a new group of tuneable photoswitches capable of responding to visible light – were developed. [42]

The architecture of DASAs is based on a donor moiety connected to an acceptor through a triene bridge (Fig. 5). Since 2014 researchers have discovered three generations of DASAs, which differ in their donor or acceptor moieties. The acceptor is mostly Meldrum's acid or 1,3-disubstituted barbituric acid in the 1st and 2nd generation, whereas in the 3rd generation acceptors are a vaster group of compounds derived from carboxylic acids. Contrarily to the acceptors, donor moieties vary between the 1st and 2nd generation, respectively: while the first-generation DASAs contain dialkylamine-based donors, the donors of the second-generation (as well as the third-generation) DASAs are *N*-alkylanilines.

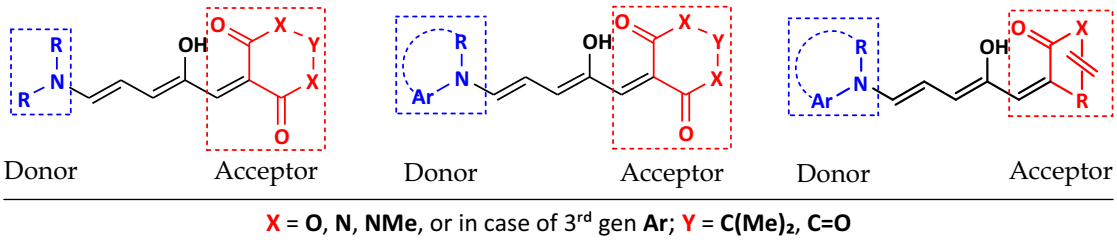

Fig. 5: Structure of donor–acceptor Stenhouse adducts of 1st (left), 2nd (middle), and 3rd generation (right).

Just like Stenhouse salt, DASA isomers are distinguishable by colour: if the solution is strongly coloured, DASA is in its open form, whereas a colourless or slightly yellow solution indicates the opposite. The triene bridge has a very strong absorption band

in the visible range corresponding to the $\pi \cdots \pi^*$ transition. In case of the 1st generation, absorption maximums are 545 nm and 570 nm determined by the acceptor Meldrum's and barbituric acid derivates, respectively, while the donor dialkylamine moiety has only little effect on the absorption maximum in units of nm. [47] On the other hand, the effect of different donor moieties is noticeable in switching properties, when with higher steric demand decreases the percentage of closed form if under light and increases the percentage of open form while in thermodynamic equilibrium.

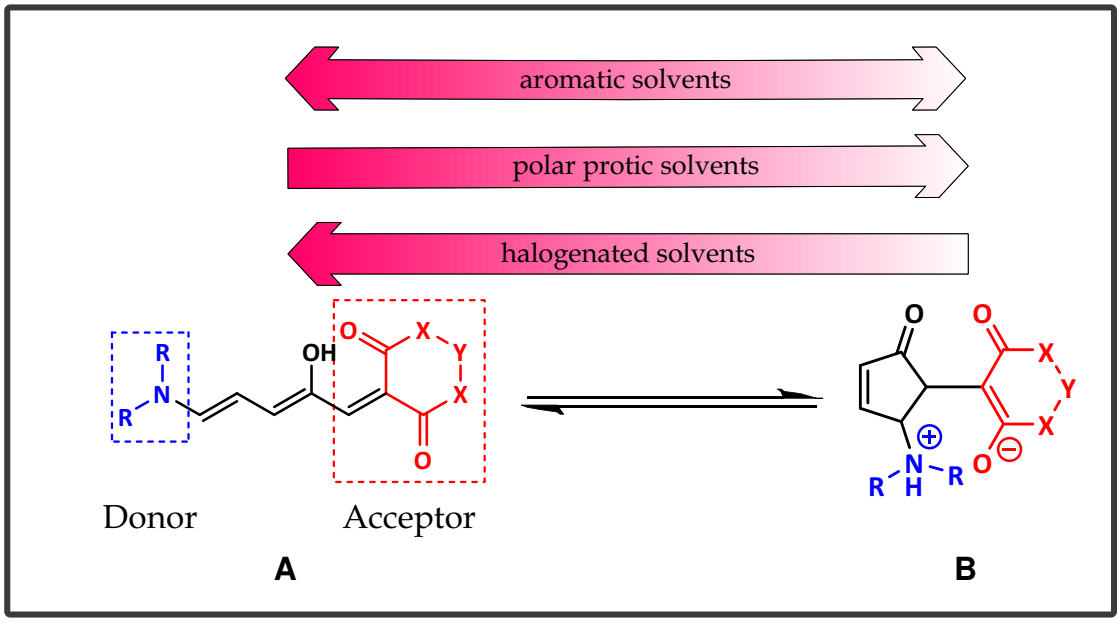

Fig. 6: Photoswitching behaviour of the first-generation DASAs depending on the solvent

Switching kinetics for both cyclisation and ring-opening are strongly dependent on the solvent, but also on other stimuli, such as light. [48] In polar protic solvents (Fig. 6), such as water or methanol, photoswitching is irreversible due to energetically advantageous zwitterionic form in them. However, in halogenated solvents, such as chloroform or dichloromethane, no or very little photobleaching is observed. In case of the first-generation DASA reversible photoswitching is observed only in aromatic solvents such as benzene or toluene. The rate of photobleaching is not identical in the relevant solvents, in protic solvents the process is much slower than eg in toluene .

3.2 Synthesis of DASA derivatives

DASAs are composed of a donor and an acceptor moiety linked through a triene bridge. [48] This modular build-up is a guiding principle for their synthesis. In the standard synthetic route of DASA, furfural reacts with the acceptor through Knoevenagel condensation. Subsequently, the fural core is opened by an aminic donor through a series of shifts akin to the (aza-)Piancatelli rearrangement resulting in the open form of DASA (**A**). Similar rearrangements are seen in DASA closure, a key element of DASA research. [42]

In order to characterise the individual generations of DASA, an examplary synthesis of each generation will be presented. In case of the 1st generation, the synthesis of the DASA analysed in this work will be described.

DASA of the 1st generation

The specific conditions for the synthesis of DASA used in this study are as follows [42, 49]: furan-2-carbaldehyde (**1**) reacts in an aqueous environment with Meldrum's acid **5** at a temperature of 75 °C for the duration of 2 hours. Consequently, the obtained yellow crystals of **6** react with the *N*,*N*-diethylamine in tetrahydrofurane at room temperature for 20 minutes yielding red crystals of the desired compound **7**. The reported yield is determined as 85% for the two-step procedure (Fig. 7).

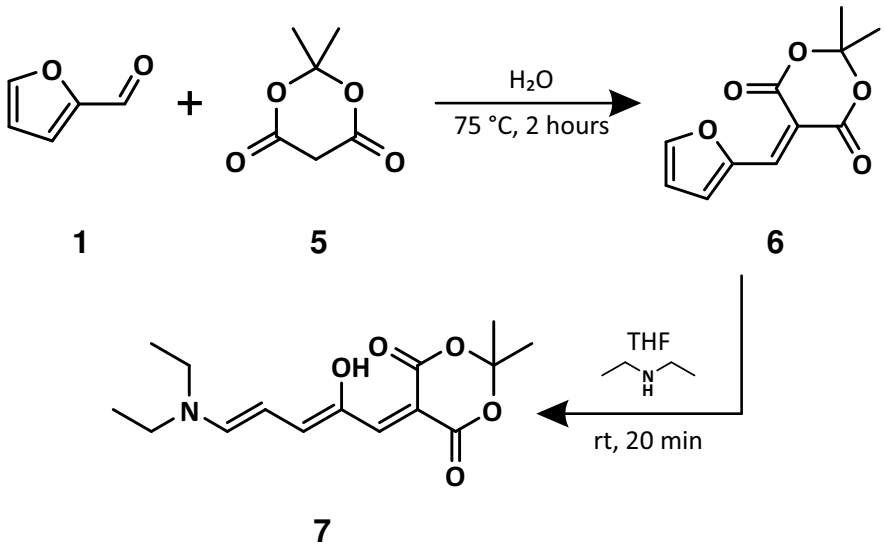

Fig. 7: An example of the synthesis of DASA studied in this work proposed by [49].

DASA of the 2nd generation

As mentioned above, the 1st and 2nd generations have common acceptor moieties: Meldrum's acid (**5**) and barbituric acid (**8**). The reaction of **1** with **5** is already presented in the previous paragraph. In the other case, **1** reacts with **8** in an aqueous environment overnight at room temperature forming a yellow precipitate of **9**. [50] Subsequently, the washed and dried product reacts with a selected *N*-alkylaniline, eg 1,2,3,4-tetraisoquinoline, in 0.4 M tetrahydrofurane at room temperuture for 10 min followed by cooling at 0 °C for 20 min (Fig. 8). [42]

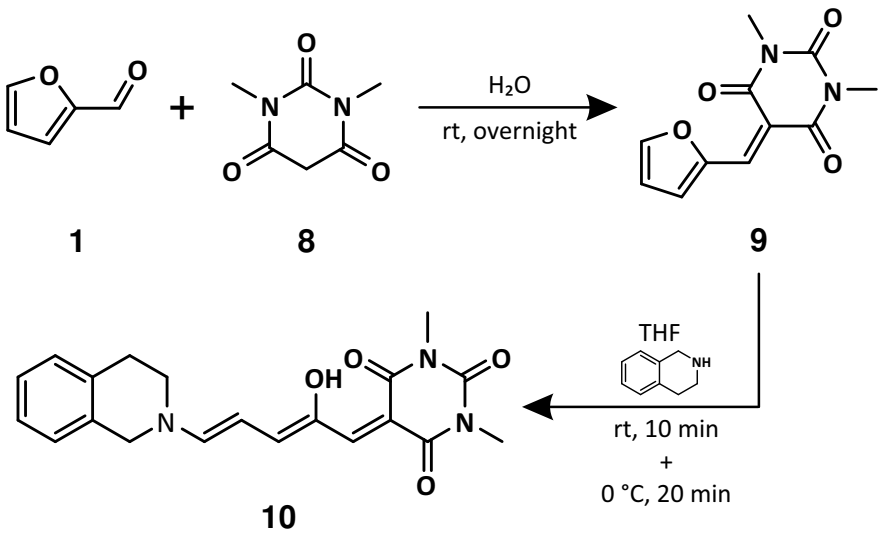

Fig. 8: An example of the synthesis of DASA of the 2nd generation.

DASA of the 3rd generation

One of the first DASAs of the 3rd generation is a compound with an acceptor base on a carboxylic acid derivative and an *N*-alkylaniline donor. Due to the wide tunability of this generation, a large palette of the compounds is used for these DASAs. The following reaction was selected as an example: **1** and carboxilic acid derivative **11** are combined in dichloromethane and stirred for 2 hours forming the product **12** (Fig. 9). [51] Subsequently, the crystals of **12** are dissolved in a minimal amount of methanol, then indoline is added and the mixture is stirred for the next 4 h. At the end of the reaction, a green powder of **13** is obtained. [52]

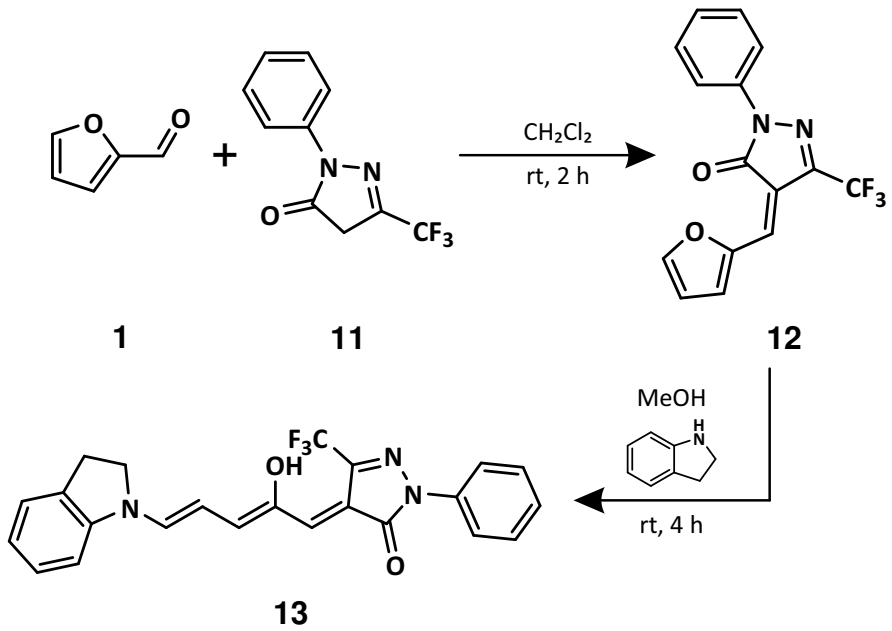

Fig. 9: An example of the synthesis of DASA of the 3rd generation.

3.3 Photoswitching mechanism

The process of photoswitching is not entirely induced by light, the whole process following irradiation can be divided into two parts: the primary photochemical and the secondary thermal process. [49] The photon absorption manifests as a $\pi \cdots \pi^*$ transition of one of the double bonds of the triene bridge. The presence of the hydroxy group seems to have an influence on the selection of the double bond [53]: DFT calculations determine the longest bond in the excited state of the molecule. In case of a molecule with a C_2-hydroxy group, the longest bond is a C_2—C_3 double bond, but in case of a missing hydroxy group the longest bond is the double bond linked to the acceptor moiety. This phenomenon preselects the C_2—C_3 bond for isomerisation **i** depicted on Fig. 10. Thenceforward, processes are of thermal nature. After the Z/E-isomerisation, the C_3—C_4 single bond rotation **ii** occurs, followed by ring-formation **iii** through conrotatory 4π-electrocyclisation, which is enabled by the proximity of C_1 and C_5. The final formation of **14** relies on a proton transfer **iv**. The intermediates differ significantly in charge, polarity, dipole moment and geometry, therefore the switching properties change from solvent to solvent.

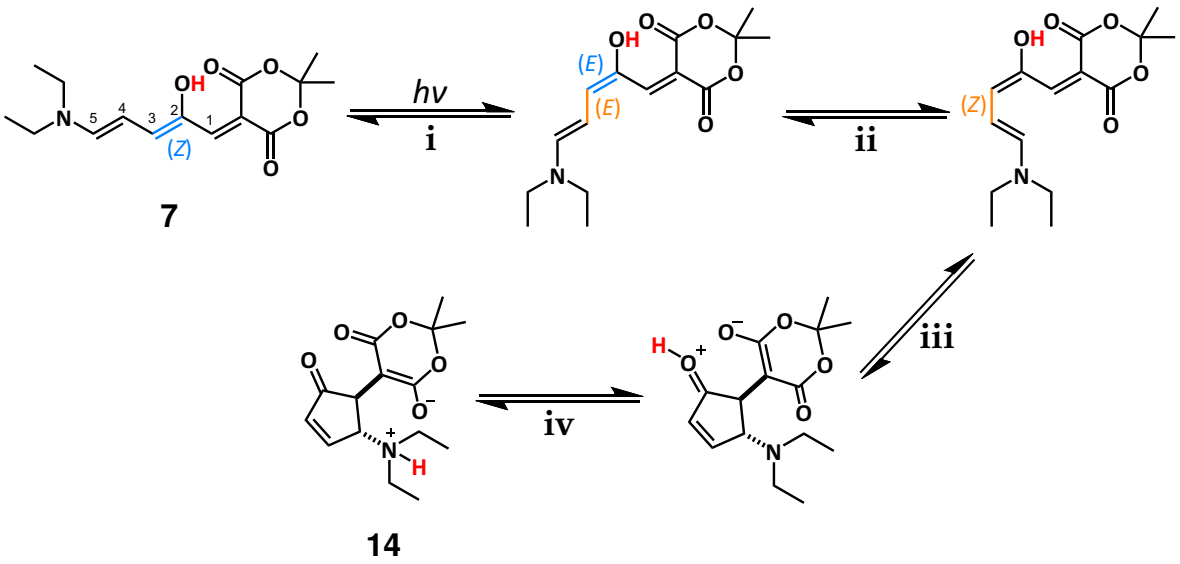

Fig. 10: The detailed process of DASA photoswitching

II. EXPERIMENTAL PART

4 PROPERTIES OF ANALYSED COMPOUNDS

The Stenhouse adduct analysed in this work was 5-((2*Z*,4*E*)-5-(diethylamino)-2-hydroxypenta-2,4-dien-1-ylidene)-2,2-dimethyl-1,3-dioxane-4,6-dione (hereinafter referred to as 'oDASA') and its closed form 5-(2-(diethylammonio)-5-oxocyclopent-3-en-1-yl)-2,2-dimethyl-4-oxo-4*H*-1,3-dioxin-6-olate (hereinafter referred to as 'cDASA'). [42] Both forms have a molar mass of 295.335 g·mol^{-1}, an exact mass of 295.142 u, and can be described by the molecular formula $C_{15}H_{21}NO_5$. Their structure and geometry is depicted on Fig. 11. The model is calculated by the software Avogadro and it shows the energetically most opportune conformer simulated in the force field MMFF94. The compound was synthesised in the Faculty of Pharmacy, University of Lisbon in Portugal by the research group of Prof. Carlos Afonso.

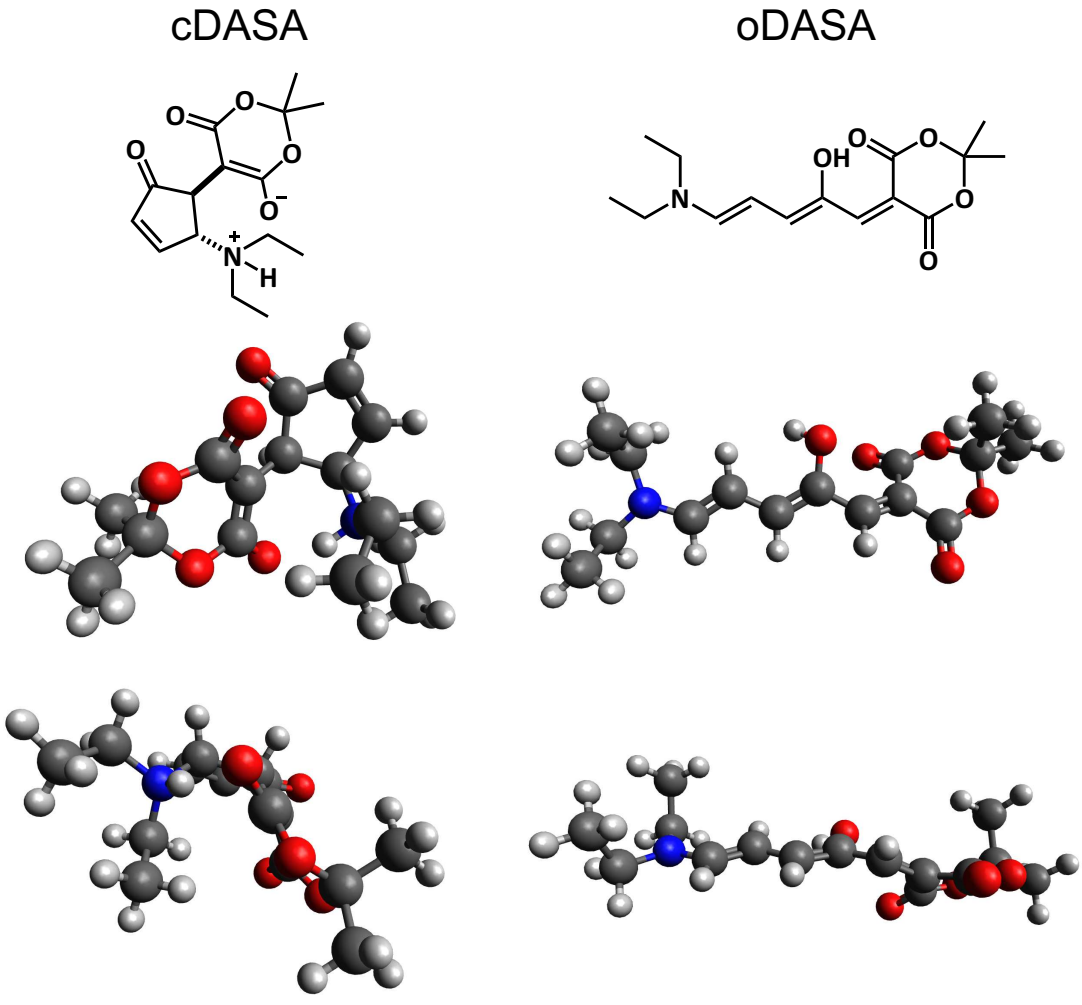

Fig. 11: The structure and geometry of the analysed compounds.

5 APARATUS AND METHODS

5.1 ESI-IT-MS experiments

5.1.1 Instrument parameters

Name:	amaZon X (Bruker Daltonics, Bremen, Germany)
Ion source:	electrospray
Mass analyser:	ion trap
Nebulising and drying gas:	nitrogen
Ion fragmentation technique:	collision-induced dissociation
Collision gas:	helium
Software:	Trap Control, Data Analysis

5.1.2 The behaviour of DASA in the gas phase

For the experiments performed on ESI-IT-MS, 10 μM solutions of DASA (closed or open form) were prepared in different solvents and their combinations. The default settings of the instrument for the analysis were the following:

Constant flow rate:	3.0 μl·min^{-1}
Electrospray voltage:	±4.2 kV
Capillary exit voltage:	±140 V
Nebuliser pressure:	55.16 kPa
Drying gas flow:	6.0 dm^3·min^{-1}
Drying gas temperature:	220 °C
ICC (positive mode):	20,000
ICC (negative mode):	7,000
Maximum accumulation time:	20 ms
Range of m/z:	50–1500

Tandem mass spectrometry experiments

In order to secure the desired form, the stock solutions of a concentration of 1.0 mg·cm^{-3} were prepared by dissolving oDASA in chloroform and cDASA in water.

The samples were prepared by diluting the stock solutions with an equiproportional mixture of methanol and water to the desired concentration. The tandem mass spectrometry experiments of oDASA and cDASA, respectively, were performed with He as the collision gas after isolating the required ions using collision-induced dissociation (CID). The other instrumental conditions, such as CID amplitude, were set for each sample individually.

The influence of the environment on the first–order mass spectra and gas-phase behaviour of DASA

In the first part of the experiment the stock solution of a concentration of 1 mg·cm^{-3} was prepared by dissolving oDASA in chloroform. The solution was consequently diluted with chloroform, acetonitrile, methanol, or water. In the second part the aqueous stock solution of cDASA was also prepared and both stock solutions were diluted by chloroform. Subsequently, 1 ml was taken from each solution and 2 μl of formic acid was added to the 1-ml samples each. The experiments were executed using the default settings of the instrument.

DASA form distiction using ESI-MS

For these experiments, two stock solutions of a concentration of 1 mg·cm^{-3} were prepared by dissolving oDASA in chloroform and cDASA in methanol, respectively. In order to observe the differences, a series of different solvent combinations were prepared. In case of oDASA, the stock solution was diluted in various mixtures of chloroform and methanol and subsequently analysed. The versions of the diluting mixture contained a rising proportion of methanol from 0 to 100% with a 10% step. In case of cDASA, the stock solution was diluted in i) pure methanol, ii) pure water, and iii) an equiproportional mixture of the two solvents. In order to confirm that methanol has the supposed influence on DASA, the series of experiments with cDASA were repeated, but the stock solution was prepared by dissolving cDASA in water. The experiments were performed using the default settings of the instrument and all samples of cDASA were prepared without any light accessing the samples.

The influence of temperature on the gas-phase behaviour of DASA

The last set of experiments focusing on the gas-phase behaviour of DASA analysed the possibility of an influence of the temperature of the drying gas on the fragmentation mechanism of the required ions. For this experiment, only the methanolic stock solution of cDASA was used. The stock solution was diluted in i) pure methanol, ii) pure water, and iii) an equiproportional mixture of the two solvents. All samples were analysed at temperatures of 25, 50, 100 and 220 °C. Except for the temperature, the default settings of the instrument were used.

5.1.3 ESI-MS analyses of mixtures of DASA with cucurbit[n]urils

For the experiments executed on ESI-IT-MS, 25 μM solutions of DASA (closed or open form) complexed with cucurbit[7]uril or cucurbit[8]uril were prepared in an aqueous or a methanolic environment. The settings of the instrument were identical to those in the previous set of experiments, only the range of m/z was changed.

5.2 NMR experiments

5.2.1 Instrument parameters

The experiments were measured on the the nuclear magnetic resonation JEOL ECZ 400 at the renonance frequency of 400 Hz. The operative temperature of the instrument was 303 K. The signals of the residual solvents were unified for ^1H NMR spectra: deuterium oxide δ 4,75 ppm, chloroform δ 7,27 ppm.

5.2.2 NMR spectra of DASA

Prior to experiments with macrocycles, ^{1}H and ^{13}C{^{1}H} NMR spectra of single oDASA and cDASA, resperctively, were measured. In this experiment, cDASA was dissolved in deuterium oxide and oDASA in deuterated chloroform in order to prevent changes in their form.

5.2.3 NMR experiments of mixtures of DASA with cucurbit[n]urils

The complex formation was investigated by titrating the guest with a solution of one of the host molecules. The initial solution of the guest was prepared by dissolving 0.8 μmol in 0.6 ml of deuterium oxide. The solution of the host was prepared by dissolving

1.28 μmol in 0.8 ml of deuterium oxide. The molar quantity of the host is defined by the final molar proportion to the guest; in the case of this experiment it is 1.6:1.
For this experiment, only ^{1}H NMR spectra were measured. Through the experiment, the molar equivalent of the host to the guest was gradually increased from 0 to 1.6 equivalent with a 0.2 eq step.

5.2.4 Competitive titration

For these experiments a solution of the complex of a concentration of 1 mM was prepared. In order to secure that most oDASA remain open and create a complex with CB[7], solid oDASA was dissolved in an exact volume of the aqueous solution of CB[7]. The preliminary calculations had to be made precisely to gain at least 0,5 ml of the solution of the complex. The ^{1}H NMR spectra were measured for the initial solution of the complex and after every addition of a 0.5 molar equivalent of the competitor, corresponding to a final 1.5 eq after three additions. Furthermore, the ^{1}H NMR spectra of the competitors and their 1:1 complexes with CB[7] were also measured.

5.3 UV-Vis spectrometry experiments

The experiments were measured on the UV/Vis spectrophotometer Specord PLUS 210 of Analytik Jena, for all the experiments the Q Quartz cuvette was utilised.

5.3.1 Kinetics of DASA and its complexes with cucurbit[n]urils

For this set of experiments 25 μM aqueous solutions of oDASA, oDASA·CB[7] and oDASA·CB[8] were prepared. Two samples were prepared for each solution, one set was kept in dark, the other in light. The UV-Vis spectra of the samples were measured every 20 minutes (in case of oDASA every 10 minutes) by spectrophotometry in the wavelength range of 200-700 nm. It is best practice to continue the measurements until the characteristic peak of the tracked compound reaches its minimum, but if necessary, the measurements can be terminated earlier.

5.3.2 Time-dependent behaviour of competitors

In this experiment tetrabutylammonium iodide and acetophenone were chosen as competitors, whose binding constants in complex with CB[7] equal to $4.1 \cdot 10^3$ [54] and $9.6 \cdot 10^3$ M^{-1} [55], respectively. An equimolar amount of one of the competitors was added to the 25 μM aqueous solution of oDASA·CB[7]. The UV-Vis spectra of the samples were measured every 10 minutes for at least 90 minutes.

5.3.3 Competitive titration

In this experiment acetophenone and dopamine were chosen as competitors, whose binding constants in complex with CB[7] equal to $9.6 \cdot 10^3$ [55] and $4.2 \cdot 10^4$ M^{-1} [56], respectively. The 100 μM aqueous solution of oDASA·CB[7] was prepared by adding an exact volume of the solution of CB[7] to the solid crystals of oDASA in order to obtain a concentrated stock solution. To ensure optimal conditions for the measurement, a 4-ml cuvette with an initial 3 ml volume of the sample of diluted 25 μM solution was used. After every measurement, the molar equivalent of the competitor was raised by 0.1 eq by adding a precisely calculated volume of the stock solution of the competitor, while correcting the molar concentration of the complex is corrected by adding the stock solution of the complex and water. The terminal molar equivalent of the competitor is 2.0 eq. For the evaluation of the experiment, UV-Vis spectra of all the compounds and their complexes with CB[7] were also measured.

5.3.4 Diffusion on the phase boundary

For this experiment a 10μM aqueous solution of CB[7] and a 10 μM solution of oDASA dissolved in chloroform were prepared. First, 4 ml of the solution of oDASA and then the same volume of the solution of CB[7] were added to two test tubes. One of the tubes was shaken for 30 seconds and the aqueous phase was analysed by UV-Vis with the wavelength range of 185–800 nm. Immediately after the measurement the analysed solution was poured back to the tube. After that, the aqueous phases from both test tubes were measured with the interval of 30 minutes. The same experiment was carried out also using toluene instead of chloroform.

III. RESULTS AND DISCUSSION

6 Introduction to the discussion section

The aim of this thesis is to discover new details about the 1st generation of donor-acceptor Stenhouse adduct (DASA). Specifically, the subject of the research was DASA composed of Meldrum's acid as the acceptor moiety and diethylamine as the donor moiety. The thesis is a contribution to the development of a mutual cooperation of the research group led by Prof. Dr. Uwe Pischel from the University of Huelva and Robert Vícha's research group at the Department of Chemistry, Tomas Bata University in Zlín.

The compound researched is one of the simplest variations of DASA, but its simplicity is not a negative feature. On the contrary, the structure appears to have a high potential for use in supramolecular chemistry. Despite the nine-year-history of DASA, only few works dealing with their supramolecular behaviour were published. Upon a review of existing articles few were found to describe the interactions of DASA with cyclodextrins and only one mentions any interaction with cucurbit[7]uril. [50] Thus it can be stated, that most of the supramolecular experiments perfomed in this study have not been described in any publications before. This thesis also holds primacy in the detailed analysis of DASA in the gas phase.

The research itself was preceded by preliminary experiments and observations in order to choose the right direction. As mentioned in the theoretical part, the behaviour of DASA strongly depends on the solvent. Following the research of Lerch [48], polar protic solvents such as water or methanol cause the compound to close, while halogenated solvents such as chloroform or dichloromethane open the DASA and keep the compound in its open form, whereas in aromatic solvents such as toluene or tetrahydrofuran DASA can switch between the open and closed forms depending on the other conditions. Although the cited research seems very clear, we arrived to conflicting results: by dissolving cDASA in methanol we obtained first a clear colourless solution, which turned into pink-red after a few minutes, indicating, that closed DASA does open in methanol and then slowly closes. This information, in the end, greatly facilitated the analysis with ESI-IT-MS.

The biggest challenge of the thesis in the planning phase was designing the NMR experiments, when we needed to create complexes with cucurbit[n]urils, which are soluble only in water, and DASA, which closes in water. The tests showed that oDASA dissolved in water closes within a few hours, therefore if the samples were prepared quickly enough, the percentage of closed oDASA would be minimal. Unfortunately, oDASA has poor dissolution rate in water even if assisted with an ultrasonic homogeniser. Considering the situation, we resigned to achieve exact molar proportions in the experiments and the solutions were prepared instead in a way to maximise the concentration of dissolved oDASA. To accomplish that, for the experiments where separate solutions of oDASA and CB[n] were not needed, the samples were prepared by dissolving oDASA in the solution of the macrocycle. The high dissolution rate of DASA is particularly noticeable in the experiments using spectrophotometry.

7 Results and discussion

7.1 ESI-IT-MS experiments

7.1.1 The behaviour of DASA it the gas phase

The ESI-MS experiments were divided into four parts, the results of which are related; the signals and differences observed in tandem mass spectrometry are also important for finding some rules to distinguish the forms of DASA using ESI-MS. It should be noted that to the best of our knowledge, there are no papers containing a detailed study of DASA in the gas phase.

Tandem mass spectrometry experiments

The aim of the first type of experiments performed by ESI-IT-MS was mainly to see, how DASAs behave in the gas phase. The results of the first examination are depicted in Fig. 13 and Fig. 12. In the first–order mass spectra several types of singly charged ions with m/z corresponding to the analysed sample were observed in positive-ion scan mode for both DASAs: protonated molecule (m/z 296), sodium (m/z 318) and potassium (m/z 334) adduct and sodium adduct of the dimer (m/z 613), meanwhile in the negative-ion scan mode only identifiable ion at m/z 294 corresponding to deprotonated molecule was observed.

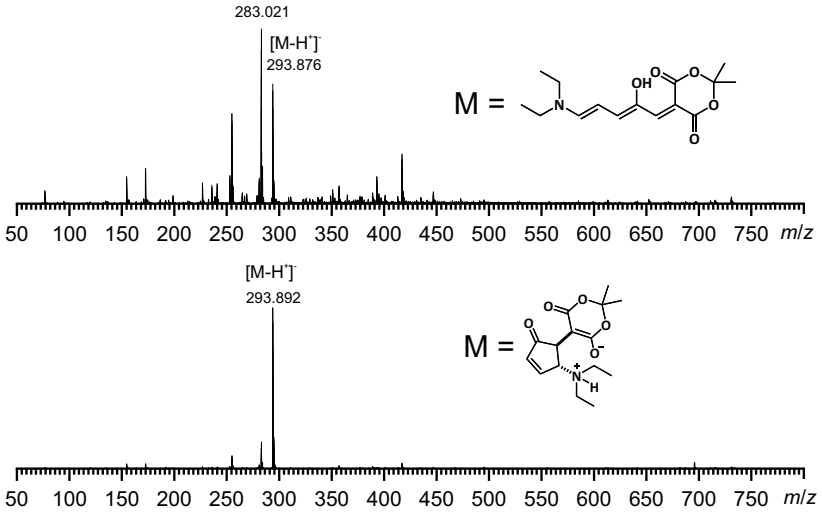

Fig. 12: ESI-MS spectra in negative-ion mode of oDASA and cDASA.

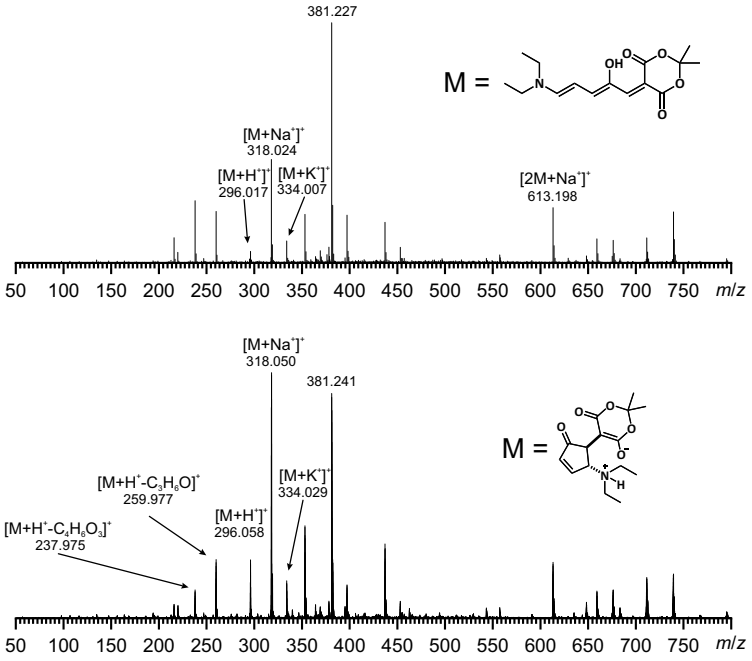

Fig. 13: ESI-MS spectra in positive-ion mode of oDASA and cDASA.

For the initial samples and the subsequent samples with similar conditions, a fragmentation mechanism is proposed based on the results. Both variations presented in Fig. 14 propose the primal fragmentation on the acceptor moiety, therefore the mechanism is valid for both forms. The mechanism is presented only for the fragment of the path, the fragmentation of DASA continues from the fragment at m/z 194 (Fig. 15), although no logical proposal for the sequent fragment was found or deducted.

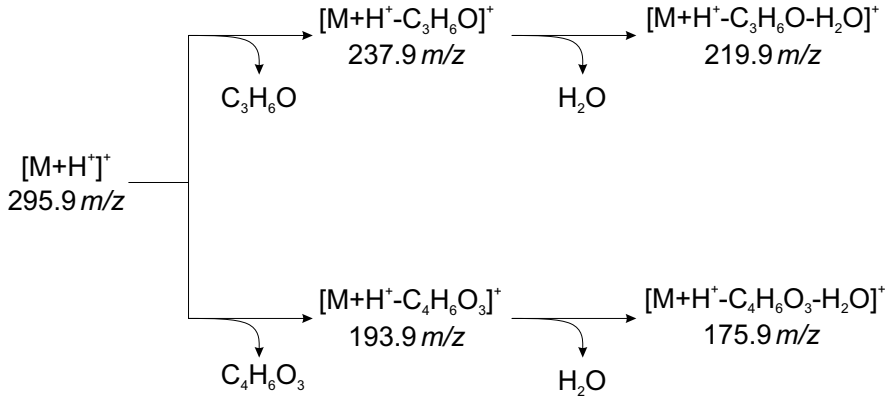

Fig. 14: A proposed fragmentation path for both forms of DASA

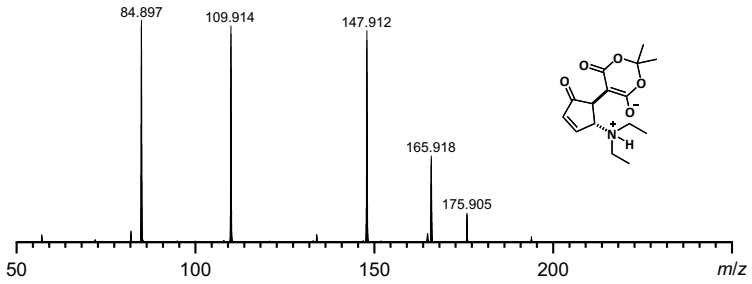

Fig. 15: $+MS^2$ of cDASA for its fragment at m/z 194

The influence of the environment on the first–order mass spectra and gas-phase behaviour of DASA

After the first tests, other solvents and combinations were analysed (Fig. 16). The solution of oDASA in chloroform was added to the different solvents. In chloroform the characteristic signals do not appear, instead the base peak was a singly charged ion at m/z 393. This signal appears in all the spectra where chloroform was used. Another set of signals was obtained from the sample prepared with acetonitrile. In the positive-ion mode a row of singly charged ions at m/z 294, 295, and 296 were detected. In case of the aqueous and methanolic samples of oDASA dissolved in chloroform, a similar result was observed as in the experiments above. The results indicate, that fragmentation is sufficient for the deeper analysis only in the presence of free available protons. In order to provide the chloroform with protons, formic acid was added to a sample and the same was done also with an aqueous sample. Unfortunately, the formic acid in tolerable quantity does not have enough influence on the fragmentation of the required ion.

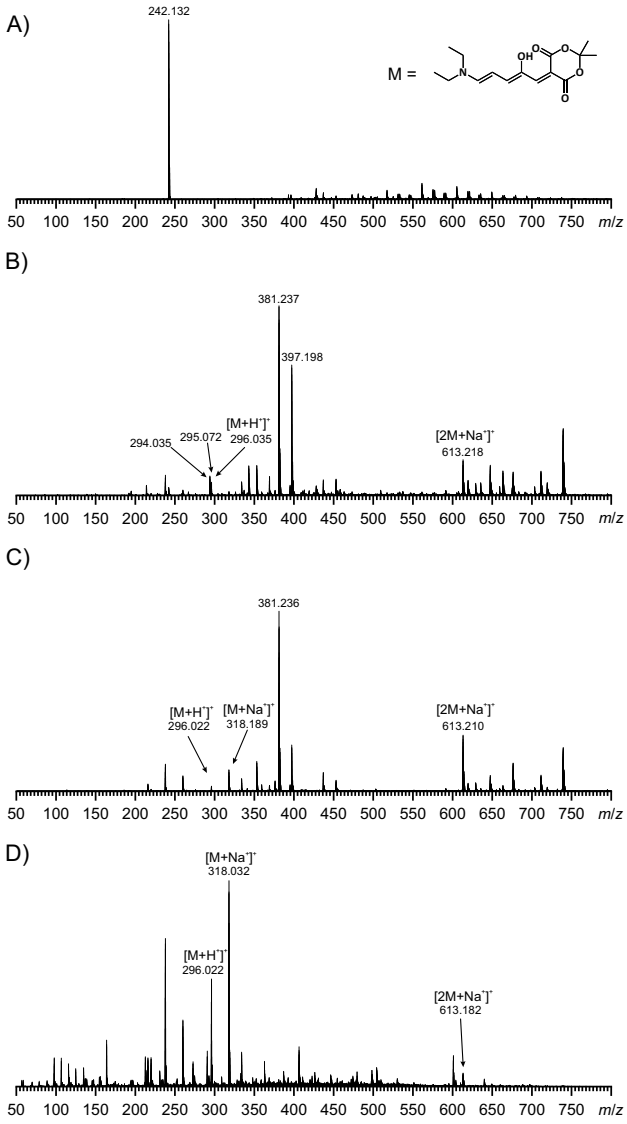

Fig. 16: The influence of a environment of a sample of oDASA on ESI-MS spectra: A) chloroform, B) acetonitrile, C) methanol, D) water

DASA form distinction using ESI-MS

This experiment required a few series of samples in order to find some rules which could be used to identify easily which form DASA is currently in. To keep it simple, the differences were searched mainly in the first-order and tandem mass spectra (MS/MS) of the required ion. Due to a high amount of artefact ions observed in the first-ion mass spectra, especially with methanol, the comparison was made for the relative intensity of peaks, which clearly originated from DASA.

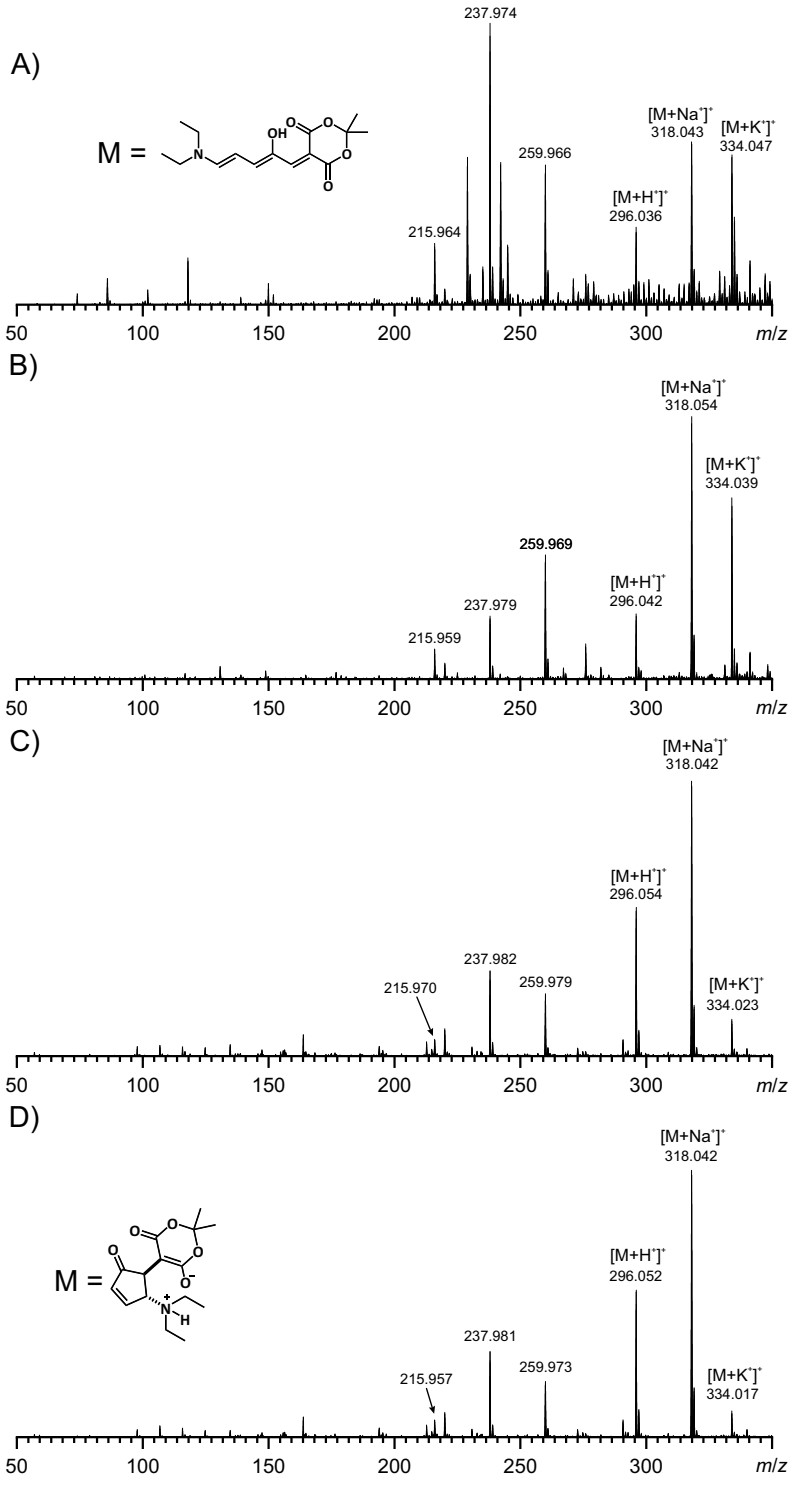

Fig. 17: +MS spectra of different ratios of oDASA to cDASA in decreasing order.

In the Fig. 17 and selected mass spectra are compared. The first noticeable difference is the ratio of sodium and potassium adducts (m/z 318 and 334, respectively). Another significant difference is the relative intensity of a singly charged product ion

at m/z 260, which is created by losing (probably) C_3H_6O (same mechanism as in Fig. 14) from the sodium adduct. The third noticeable difference is the increasing intensity of the protonated molecule together with the increasing probability of cDASA. From the first-order mass spectra the following can be also deduced: with the higher percentage of oDASA, the ion at m/z 216 becomes more intensive. This ion stems from the fragmentation of the ion at m/z 260^+ and therefore from the sodium adduct of the molecule. Another big difference between the spectra is also in the intensity of the ion at m/z 238, but based on the obtained data, the influence is more solvent-dependent than form-dependent. Tandem mass spectrometry does not show any utility, most of the differences seem to be either a solvent-dependent phenomenon, or too tiny to be used to define anything.

In the negative-ion first–order mass spectra in Fig. 18 it could be possible to deduct a few dependencies, but none of them was so evident as in the positive mode.

The influence of temperature on the gas-phase behaviour of DASA

The main scope of this section is to determine the optimal thermal conditions for the ESI-experiments with DASA. As mentioned above, in methanolic solutions a high quantity and intensity of artefacts (not originating from the analysed samples) is present. Generally, it can be assumed that lower temperatures are more suitable for ESI-MS experiments, especially for the methanolic samples. At the temperature of 50 °C the relative intensities of artefacts were minimal in the first–order mass spectra. At the lower analysed temperature of 25 °C artefacts were even less intensive in methanolic samples, although in the aqueous samples the lower temperature left more fragmented spectra (Fig. 19).

Another point of view to the evaluation of the experiment is how the temperature influences the distinguishability of the two forms. Following only the outcome of the previous experiment, differences in the intensities of ion at m/z 334^+ are noticeable only at 220 °C. Contrarily, the relative intensity of the protonated molecule is reliable in all the cases, same as the ion at m/z 238.

The results of this experiment are valuable for the further research, although in order to confirm the deduction and eliminate a possible influence of the solvent it would be useful to analyse cDASA dissolved in methanol and analyse the same sample through

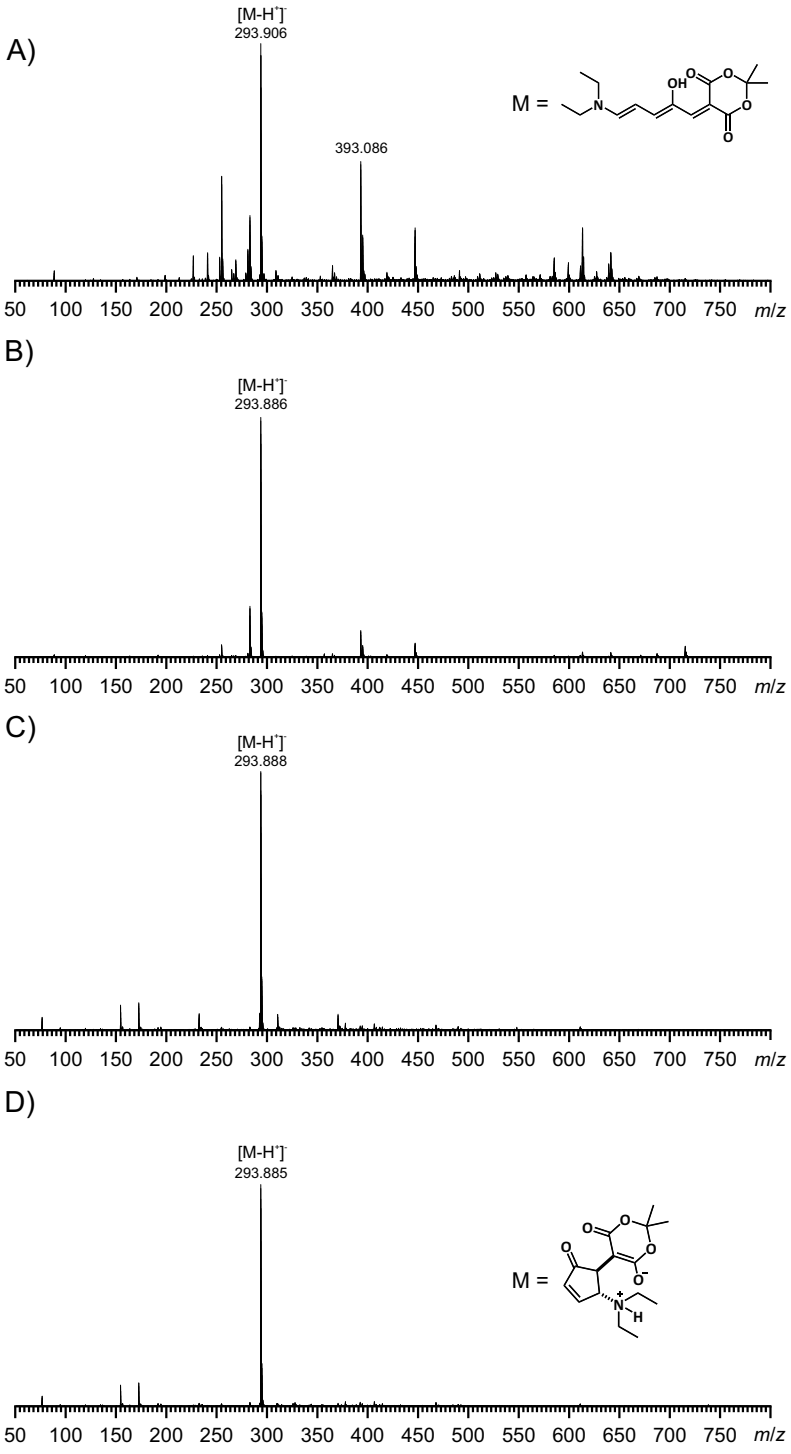

Fig. 18: -MS spectra of different ratios of oDASA to cDASA in decreasing order.

time until it completely loses the pink-red coloration (observations once a week should suffice).

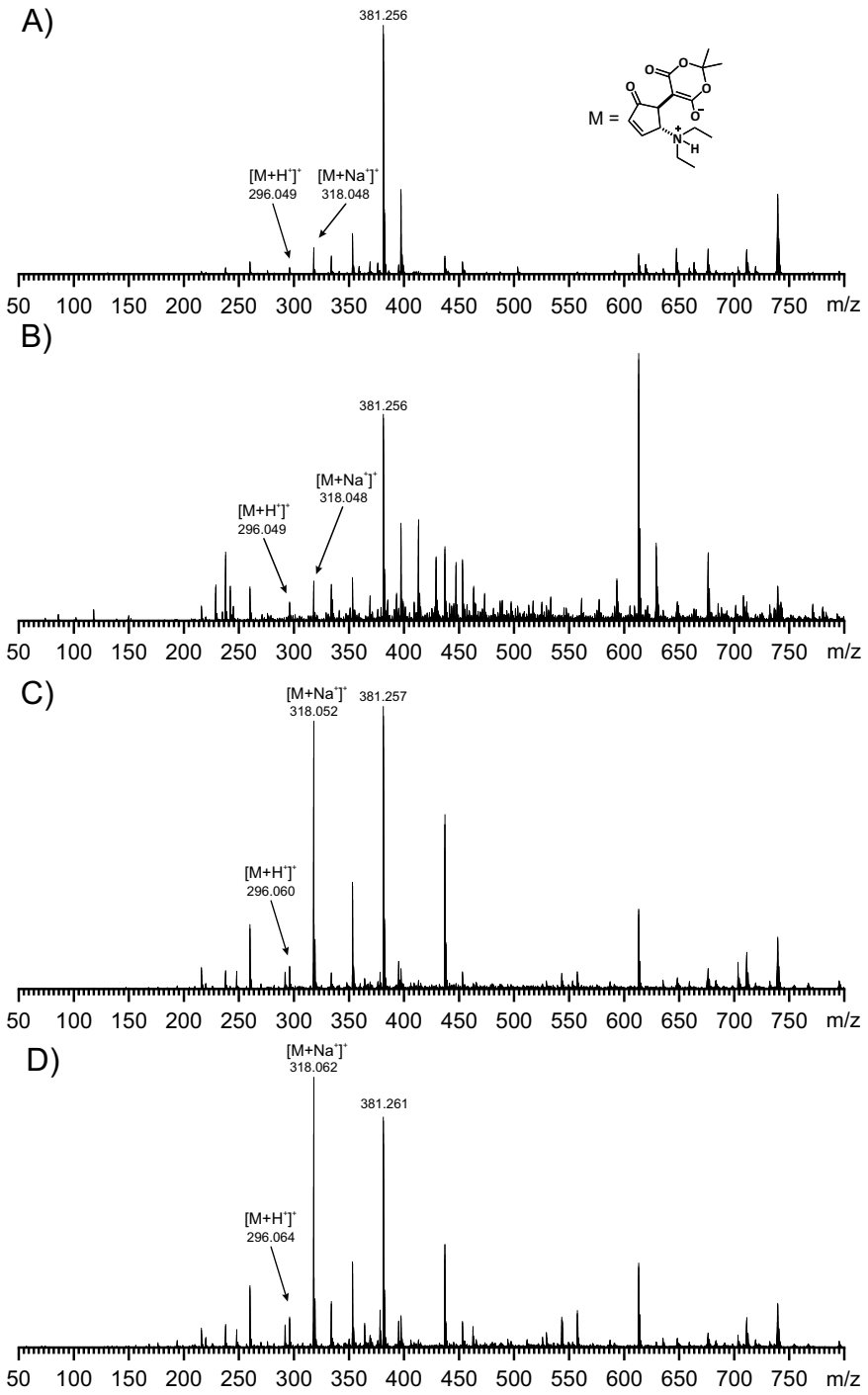

Fig. 19: The influence of temperature on the +MS spectra of cDASA: A) 220 °C, B) 100 °C, C) 50 °C, D) 25 °C

7.1.2 ESI-MS analyses of mixtures of DASA with cucurbit[n]urils

The experiments analysed the possibility to observe and eventually find use for any assay for the samples of DASA in combination with CB[n]s, unfortunately no signals of CB[7] or CB[8] neither any signals of the complexes were detected. In all the

experiments with CB[n]s, only signals of DASA were detected, and in case of a methanolic sample, probably a signal of the complex of CB[7] with the artefact 381^{+} was detected.

7.2 NMR experiments

7.2.1 ^{1}H NMR spectra of DASA

The signals of ^{1}H NMR spectra for both oDASA and cDASA were assigned to single hydrogens or in case of uncertain identification to a group of hydrogens by interpreting the ^{1}H NMR spectra.

^{1}H NMR spectrum of cDASA measured in deuterium oxide (Fig. 20) presents two intense signals in the aliphatic area, which are suitable as a reference for other signals. The only groups of multiple aliphatic hydrogens are two pairs of methyl groups (indicated by red and green dots). The integral values of both signals are similar, therefore the relative integral values of both signals equal to 6 corresponding to six protons each. The multiplicity of the two signals implies that the triplet belongs to the protons of ethyl group (green dots) and the singlets belong to the protons of methyl groups on the acceptor moiety. Through the integral ratios other signals were also identified. A broad signal at 3.34 ppm with integral intensity of 4 belongs to CH_2 of the ethyl groups (yellow dots) and the remaining signals, all of intensity 1, belong to the protons of the furan core. Obtaining more detailed identification would require at least COSY spectrum, but preferably also a spectrum of carbon nuclei as well as a heteronuclear 2D spectrum.

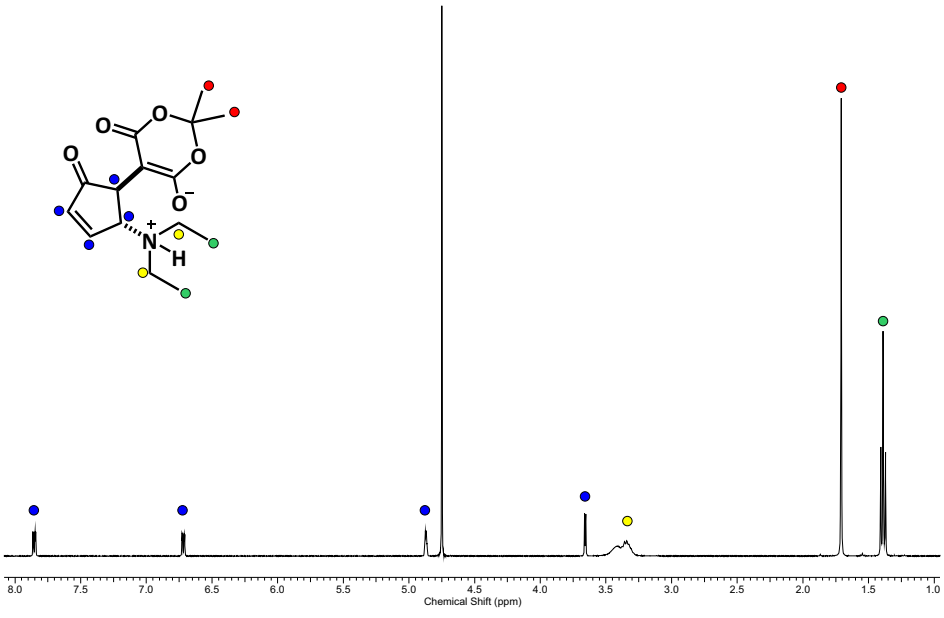

Fig. 20: ^{1}H NMR spectrum of cDASA measured in D_2O

The signals of ^{1}H NMR spectrum of oDASA measured in chloroform were analysed with analogue logic as in case of cDASA (Fig. 21). The singlet of methyl groups of the acceptor was chosen as the reference peak, subsequently the protons of the ethyl group were succesfully identified from the multiplicities and integral ratios, despite the impurities. The group of four signals of integral ratio 1 belongs to the protons of the triene bridge and the deshielded singlet belongs to a proton of the hydroxy group. Even more important than the spectrum of oDASA in chloroform, would be its spectrum in an aqueous environment for all the NMR experiments of this thesis. However, in an aqueous environment the process of ring-closing of oDASA begins immediately, therefore two sets of signals are noticeable in 1H NMR spectra (Fig. 22). By identifying all signals of cDASA it is possible to isolate the signals of oDASA and focus only on them in the subsequent experiments. By comparing the ^{1}H NMR spectrum of oDASA and cDASA the undesirable signals were excluded (black dots).

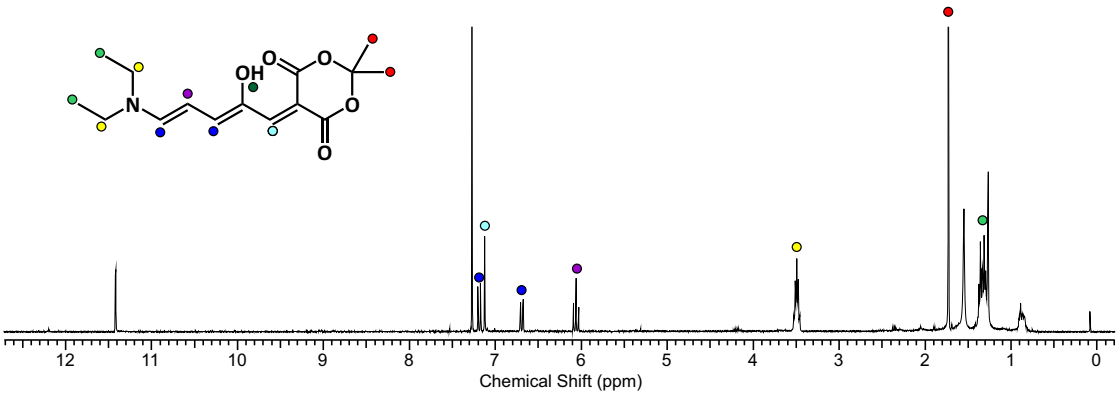

Fig. 21: ^{1}H NMR spectrum of oDASA measured in chloroform

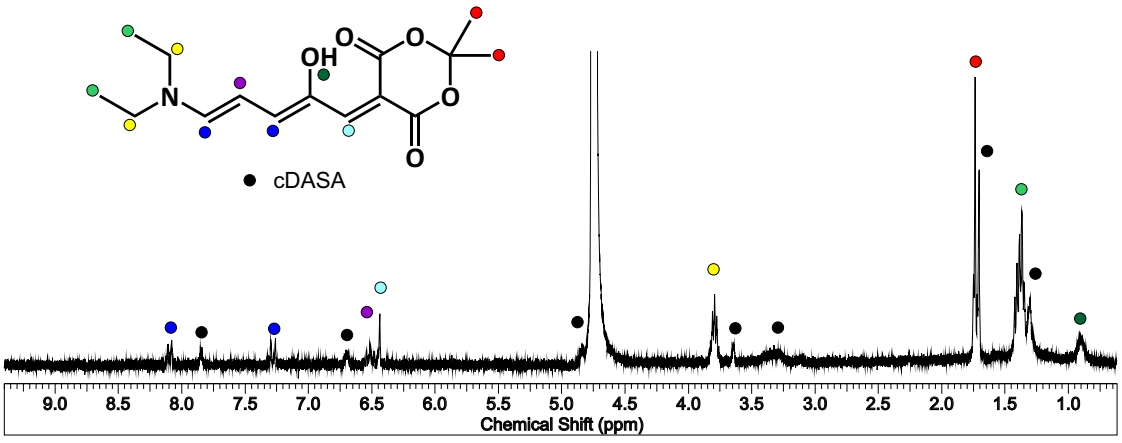

Fig. 22: ^{1}H NMR spectrum of cDASA measured in D_2O

Due to a low concentration of oDASA, the integral intensities were too inaccurate, therefore only following the shifts, gross intensity and multiplicity of the signals were used to identify the signals. The multiplet and singlet in the aliphatic area belong to protons of methyl (red dots) and CH_3 of ethyl groups (green dots). The CH_2 of ethyl groups have the multiplet near to the signal of the solvent. In the aromatic area, two doublets, a triplet and a singlet were identified and assigned.

7.2.2 NMR experiments of mixtures of DASA with cucurbit[n]uril

For this experiment, four sets of the measurements were performed. The experiments were planned in order to confirm or deny the hypothesis and the mathematic models presented in previous subchapter.

In the Fig. 23 the comparison of the ^{1}H NMR spectra is presented. Through the experiment, new sets of signals appeared, although the signals of cDASA are noticable at any concentration of CB[7]. The new set of signals is in close proximity to the easily accessible protons, the multiplicity of the new signals corresponds to them. Presumably, cDASA creates a sort of external complex with CB[7] as the mathematical models suggest. This assumption also follows the interactions of easily accessible protons with CB[7] noticeable in the spectra.

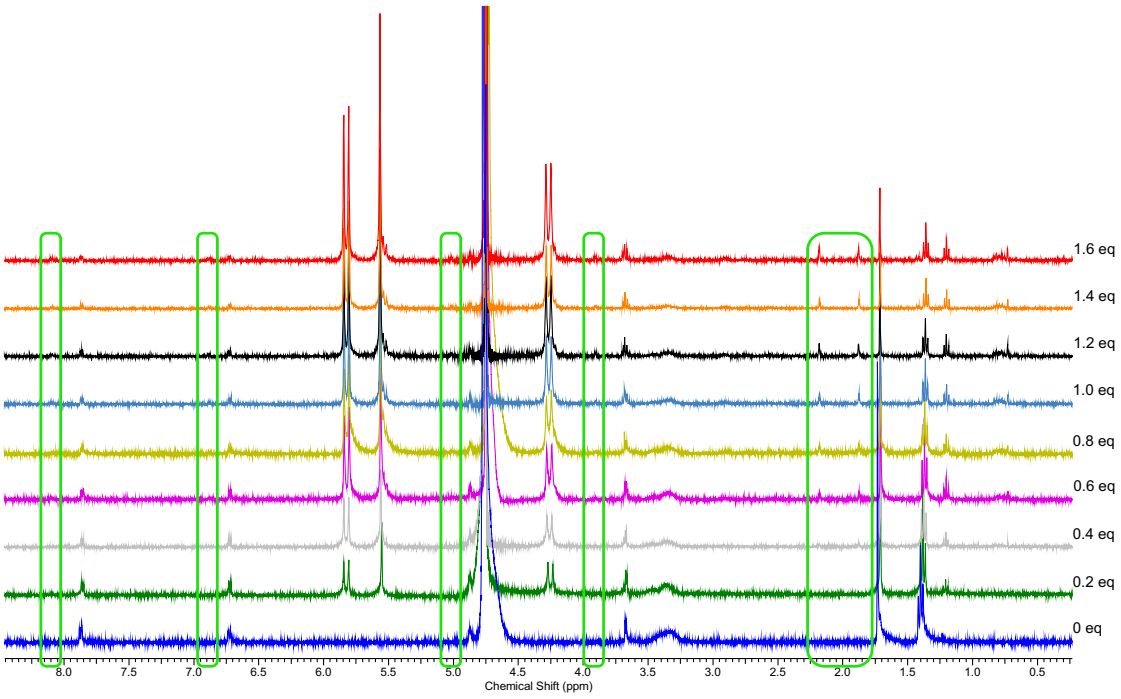

Fig. 23: ^{1}H NMR spectra of titration of cDASA with CB[7]

In case of the complex of cDASA with CB[8] in Fig. 24 the situation is similar. The spectra clearly dismiss any speculations about internal complexation. In the spectra only one new set of signals ascends, although other small signals might be hidden in the noise. The new set of signals confirms the formation of simulated weak external complexes.

A different scenario happens in case of the mixture of oDASA with CB[7] (Fig. 25). Up

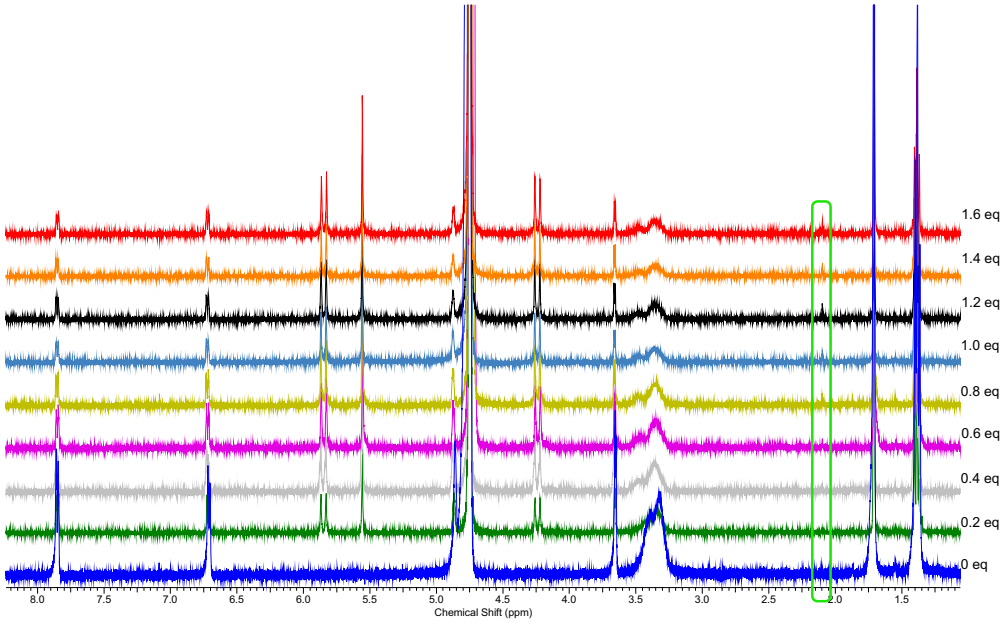

Fig. 24: ^{1}H NMR spectra of titration of cDASA with CB[8]

to 0.4 eq there are noticeable shifts of the most signals of oDASA. From the experiment it seems, that the equilibrium is reached after the 2nd addition. Even though this result could indicate, that the stoichiometry of the complex is 2:1, probably this suggestion is not right: due to problems with the preparation of the solutions mentioned before, the solution of the guest was significantly less concentrated than calculated and the molar equivalent of the host was higher. In the spectra the signals of cDASA are also clearly identifiable. The most noticeable change in intensities is at the signals of the donor moiety. The simulations imply, that the most probable complex oDASA@CB[7] is made by the interaction of the donor moiety inside the cavity. The last combination, oDASA with CB[8] (Fig. 26), also shows some shifts, but mostly for the signals of the donor moiety. The stoichiometry of the complex is, despite the spectra, probably 1:1, because of the same complications as in case of CB[7]. To summarise this set of the

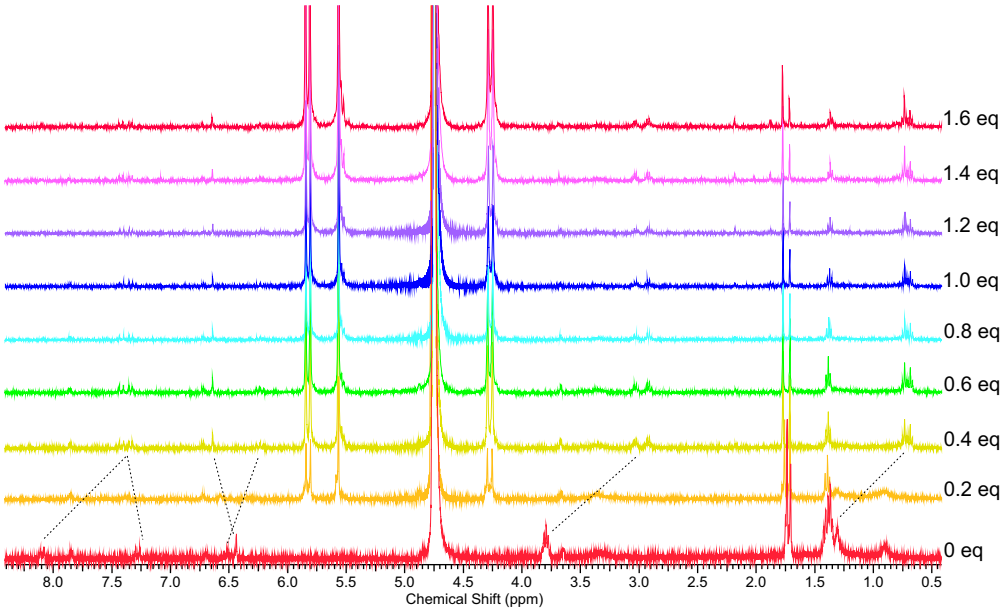

Fig. 25: ^{1}H NMR spectra of titration of oDASA with CB[7]

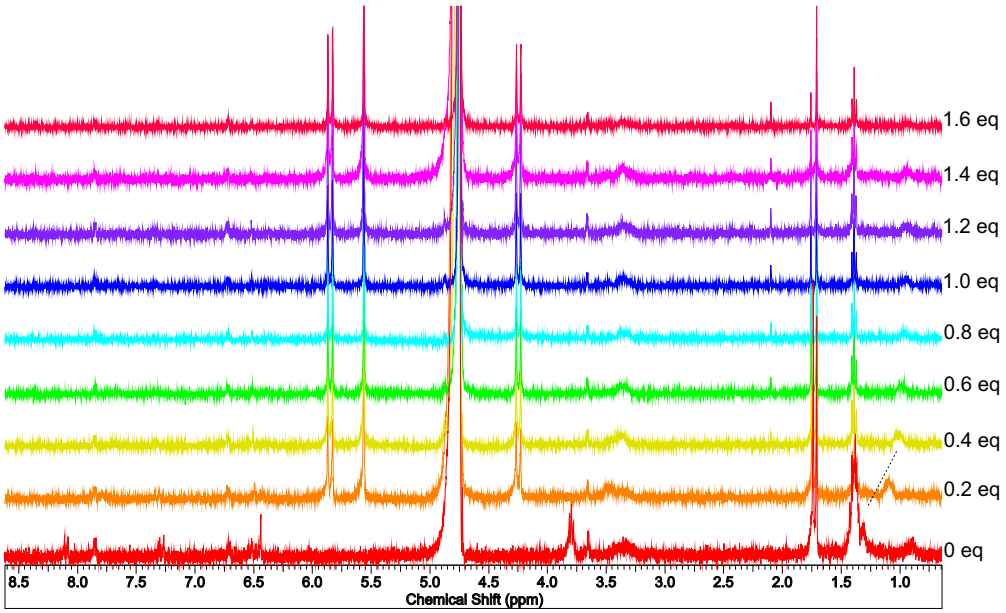

Fig. 26: ^{1}H NMR spectra of titration of oDASA with CB[8]

experiments, the analysed DASA creates internal complexes only in its open form and the most stable and prospective is the complex oDASA@CB[7].

7.2.3 Competitive titration

Taking the results of the preceding experiments into consideration, the following experiments are executed only with complexed oDASA@CB[7]. The competitive titrations analysed by ^{1}H NMR were executed with acetophenone and dopamine as

competitors (their ^{1}H NMR spectra are presented in Fig. 27). Due to the unknown exact concentration of the complex in the initial solution, the difference in molar equivalents between the single measurments was higher than in case of the previous experiments. The first competitor, acetophenone, is distinguishable in ^{1}H NMR

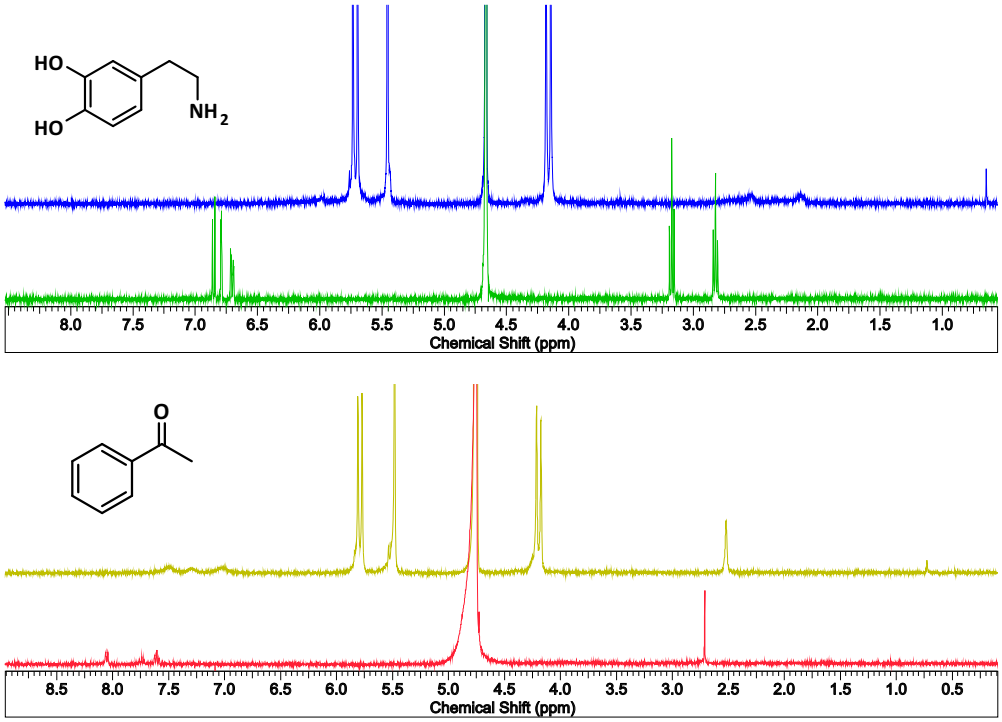

Fig. 27: ^{1}H NMR spectra free and complexes competitors (above dopamine, below acetophenone

spectrum by a trio of signals in the aromatic area and an aliphatic singlet (Fig. 28). The signals of oDASA@CB[7] in all three measurements do not shift, the only change is in the signals of acetophenone. Eventually a small signal of cDASA appears due to spontaneous actions unrelated to the presence of the competitor.

The opposite situation happened in case of dopamine in Fig. 29. Immediately after the first addition of the competitor the signals of isolated oDASA were noticeable and after the second addition broad signals of complexed dopamine also appeared.

As the result of the experiment is possible to approximate the binding constant of oDASA complexed with CB[7]. The experiments place the binding constant in the interval between the binding constant of acetophenone and dopamine.

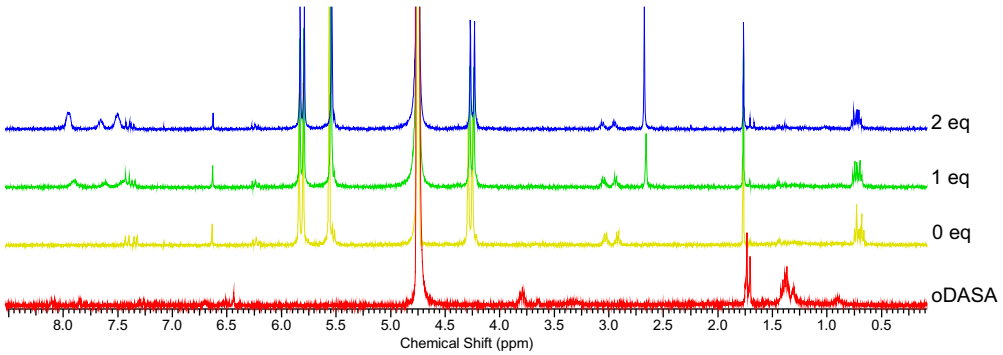

Fig. 28: ^{1}H NMR spectra of a competetive titration of complex oDASA@CB[7] with acetophenone

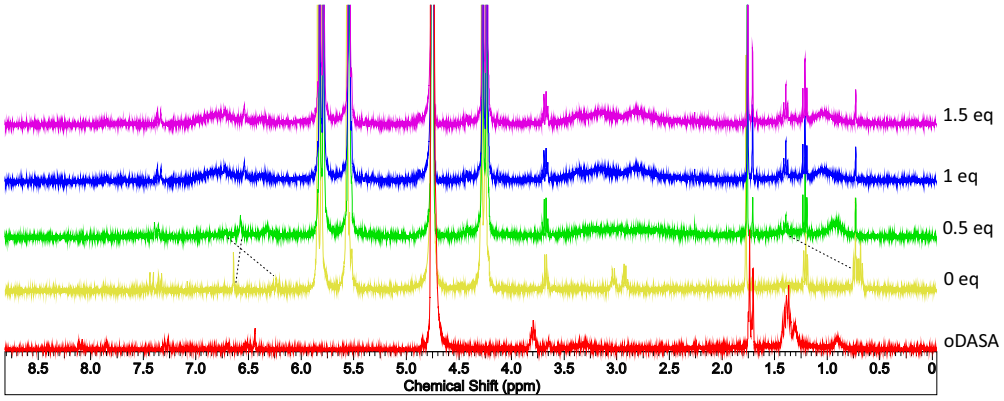

Fig. 29: ^{1}H NMR spectra of a competetive titration of complex oDASA@CB[7] with dopamine

7.3 UV-Vis spectrometry experiments

Before the experiments itself the spectra of the compounds and their complexes with CB[7] were analysed in order to define their characteristic peaks (Fig. 30). The parallel use of UV-Vis spectrophotometry is in this case useful. The method is capable of analysing the sample at a lower concentration. Adittionally, the measurments itself are much faster, therefore for any experiments tracking changes spectrophotometry should be preferred in the first place at least for the preliminary experiments.

7.3.1 Closing kinetics of DASA and its complexes with cucurbit[n]urils

The experiments show the effect of complexation of oDASA with CB[7] and CB[8], respectively. The expected outcome is slowing down the closure of the DASA molecule. As the NMR experiments and mathematic models have shown, CB[7] forms more stable complexes with oDASA than CB[8], therefore better results are expected in case of the

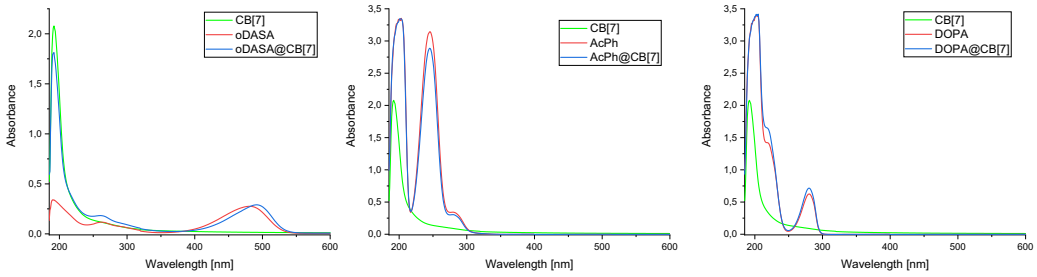

Fig. 30: UV-Vis spectra of free and complexed compounds (DOPA = dopamine, AcPh = acetophenone).

complex oDASA@CB[7]. In Fig. 31 the effect on DASA is clearly noticeable , whose closure trend is presented in Fig. 32. The negative influence is also remarkable in case of

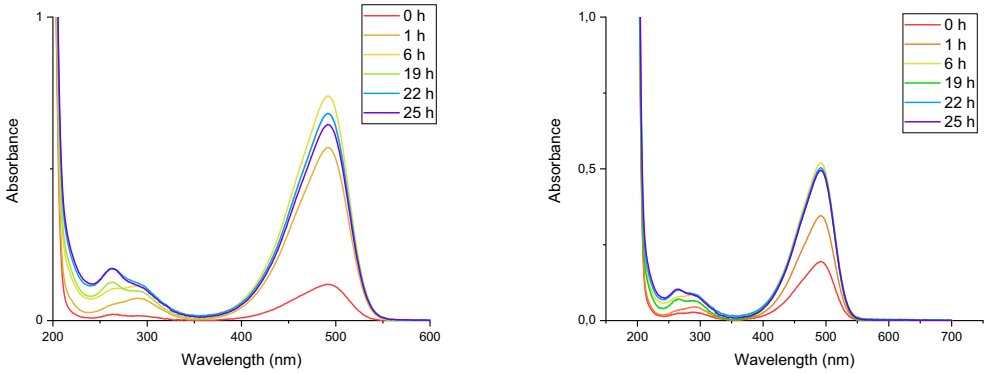

Fig. 31: UV-Vis spectrum of closing kinetics of oDASA@CB[7] with (left) and without (right) the access to light.

CB[8] in Fig. 33, however significantly weaker than in case of CB[7]. The complications with the solubility rate of oDASA in water are described in the introduction. The experiments prove the statement, because in all cases only after a few hours the maximal concentration of oDASA@CB[7] was reached. Therefore the trends were analysed after reaching the maximal concentration.

7.3.2 Time-dependent behaviour of competitors

The first competitive experiment measured by spectrophotometry was an observation of the time-dependent behaviour of competitors in the presence of oDASA@CB[7].

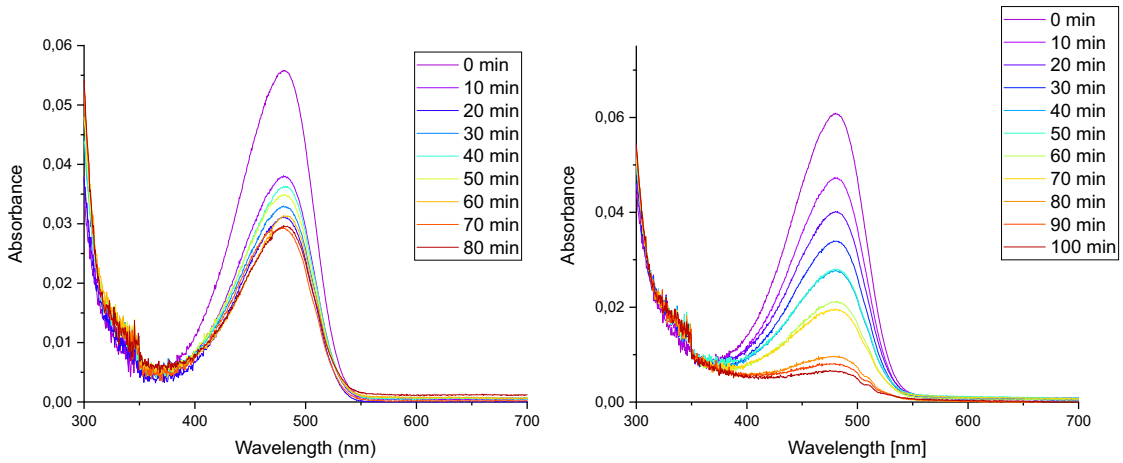

Fig. 32: UV-Vis spectrum of closing kinetics of oDASA with (left) and without (right) the access to light.

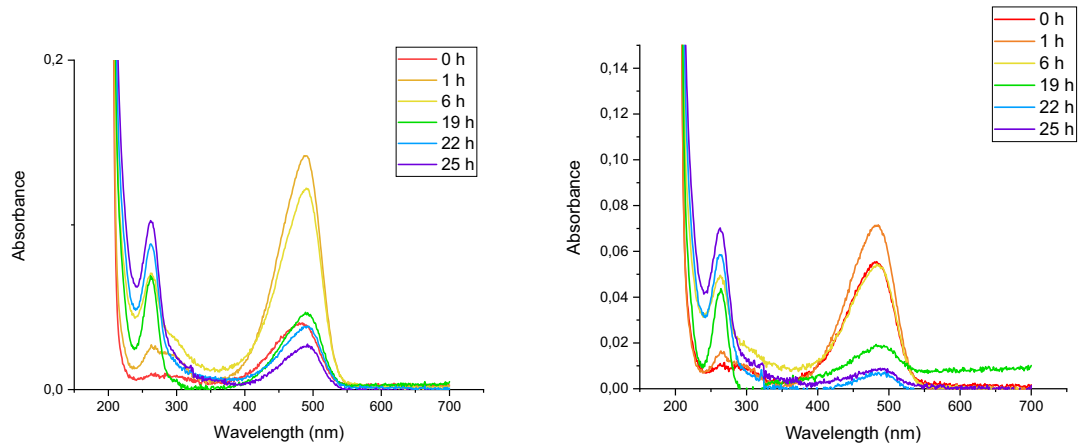

Fig. 33: UV-Vis spectra of closing kinetics of oDASA@CB[7] with (left) and without (right) the access to light.

Neither tetrabutylammonium iodide (TBAI) or acetophenone demonstrated the ability to compete with oDASA. In both cases the trend was identical: through time the concentration of the complex was decreasing and proportionally to it the concentration of the competitor was also declining (see Fig. 34). The phenomenon, however, was not caused by the competition, but by the closure of oDASA, due to which free CB[7] was available for complexation with the competitors. The scenario, where the competitors induced the decomplexation would be noticeable not only by the 'natural' decrease of the concentration, but the peak at 491 nm would be shifting towards lower values, concretely to 461 nm, where the absorption maximum of oDASA lies.

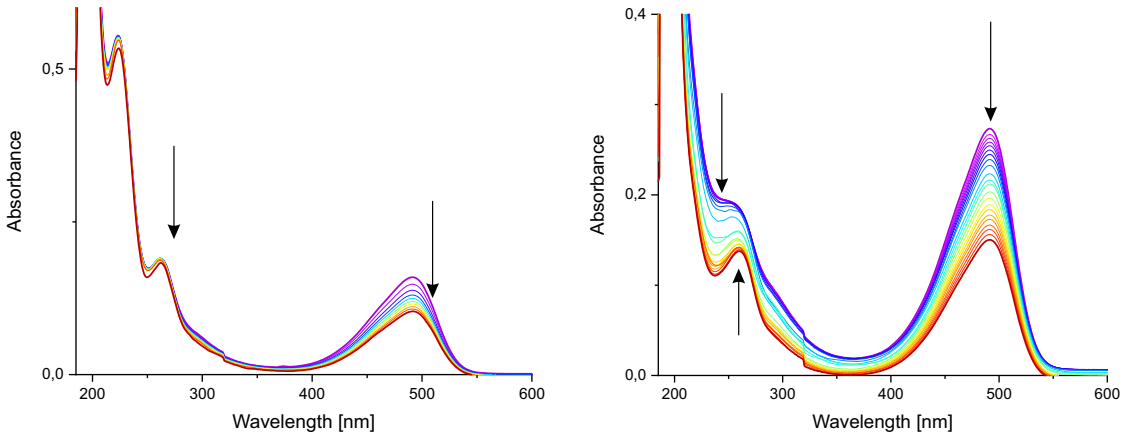

Fig. 34: UV-Vis spectra of measured kinetics of oDASA@CB[7] in presence of tetrabutylammonium iodide (left) and acetophenone (right).

Because of the lower binding constant with CB[7] of TBAI in comparison with acetophenone, in subsequent experiments only acetophenone was used and another competitor with a higher binding constant, dopamine, was chosen.

7.3.3 Competitive titration

The spectra in Fig. 35 present the results of the competitive titrations of oDASA@CB[7] with the competitors acetophenone and dopamine. In the first case, according to the previous results, titration with acetophenone should not cause any shifts in the characteristic peaks of oDASA. Considering the changes in the spectra, the supposition was confirmed. The peak at 491 nm, the characteristic peak of the complex oDASA@CB[7], is slowly decreasing due to the closure of oDASA induced by light and an aqueous environment. Consequently, free CB[7] creates complexes with the available acetophenone causing an increasing peak at 248 nm. Even though it seems, that the peak at 261 nm is shifting towards lower values, in reality it is probably slightly growing, but the changes are fused into the superposition of the neighbouring peaks. The expected shift, however, is observable in the spectra of titration with dopamine, even though the shift is not noticeable on the first sight. In Fig. 35 the peak rises at 261 nm and the absorption of the wavelengths rises in proximity of 220 nm, which is characteristic for the formation of complex of dopamine with CB[7]. Simultaneously the peak decreases initially at 491 nm while it is slowly shifting towards lower wavelengths. The shift is highlighted in Fig. 35.

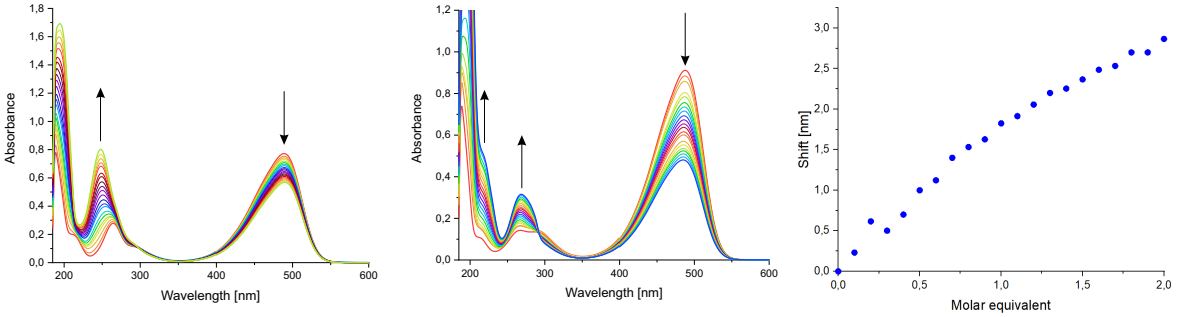

Fig. 35: UV-Vis spectra of competitive titration of oDASA@CB[7] by acetophenone (left) and dopamine (middle) and the graphical depiction of the shift of the peak initally at 491 nm (right).

The set of the experiments measured by spectrophotometry corresponds to the results from NMR experiments. But in contrast with NMR, due to the higher sensitivity of spectrophotometry, the results were of better visual quality despite the lower financial load.

7.3.4 Diffusion on the phase boundary

This subchapter presents the experiment examining a possibility to create a complex oDASA@CB[7] on the phase boundary between the halogenated or aromatic solvent with stable oDASA and an aqueous solution of CB[7]. The hopes lied in finding a manner to control the concentration of the complex thus enabling to use direct methods to determine the binding constant of the complex.

The first experiment was executed using a solvent with higher density than water, specifically dichloromethane. Regardless whether the test tube was shaken before or not, the complexation on the boundary merely happens. Therefore, another solvent was tested, this time with lower density than water, namely toluene. At the beginning it seemed promising, the shaken test tube contained a slightly coloured aqueous phase. The spectra show the initial growth, although after a few hours oDASA isomerised into its closed form.

Even though the experiment does not seem to have a positive outcome, the velocity of the assisted complexation through the phase boundary should be noticed and other experiments should be done, eg shaking by a high-frequency machine in dark and with

different solvents. Helmy in his paper [42] describes the transfer between the phases and some variations of DASA reach nearly 100% transfer to aqueous phase.

7.4 Mathematical models

As a part of the preliminary analysis, some mathematical models were simulated. By using the XTB sidocking module (XTB software version 6.6.0), a set of binary complexes was created. The fifteen best-rated structures (according to the predicted binding energy, -ΔGbind) were further optimized using the semi-empirical DFT "tight binding" approach with the GFN2-xTB method (XTB software version 6.6.0), including the effects of H2O as an implicit solvent using the ALPB model. The selected optimized structures were further optimized using DFT B97-3c/def2-mTZVP with dispersion correction D3BJ (ORCA software version 5.0.4) with an implicit solvent (CPCM). To verify that the structures were indeed at a local minimum, vibrational spectra were calculated and checked for imaginary frequencies. The approximate stability of the complexes was assessed based on the difference in total energies ($E_{bind} = E_{complex} - E_{host} - E_{guest}$). The conclusion from the simulations is the following: the only inclusive complex predicted was the open DASA with CB[7]. Additionally, the binding energy rose three times if oDASA was in the protonated state. The complex was created only in case of 'fully opened' DASA, therefore after the Z/E-isomerisation of oDASA the complexation did not occur and only weak interactions with the portals of CB[7] were calculated. The other combinations did not result in the internal complexation, however external complexes were being created between cDASA and both CBs. Weak ion-dipole interactions were predicted between the donor moiety of cDASA and the portal of the macrocycles. The last combination, oDASA with CB[8] also created external complexes with partial inclusion into the cavity, but the interactions were so weak, that it was not sure, if some kind of a bond was being created. The most representative mathematical models of some complexes are presented below in Fig. 36.

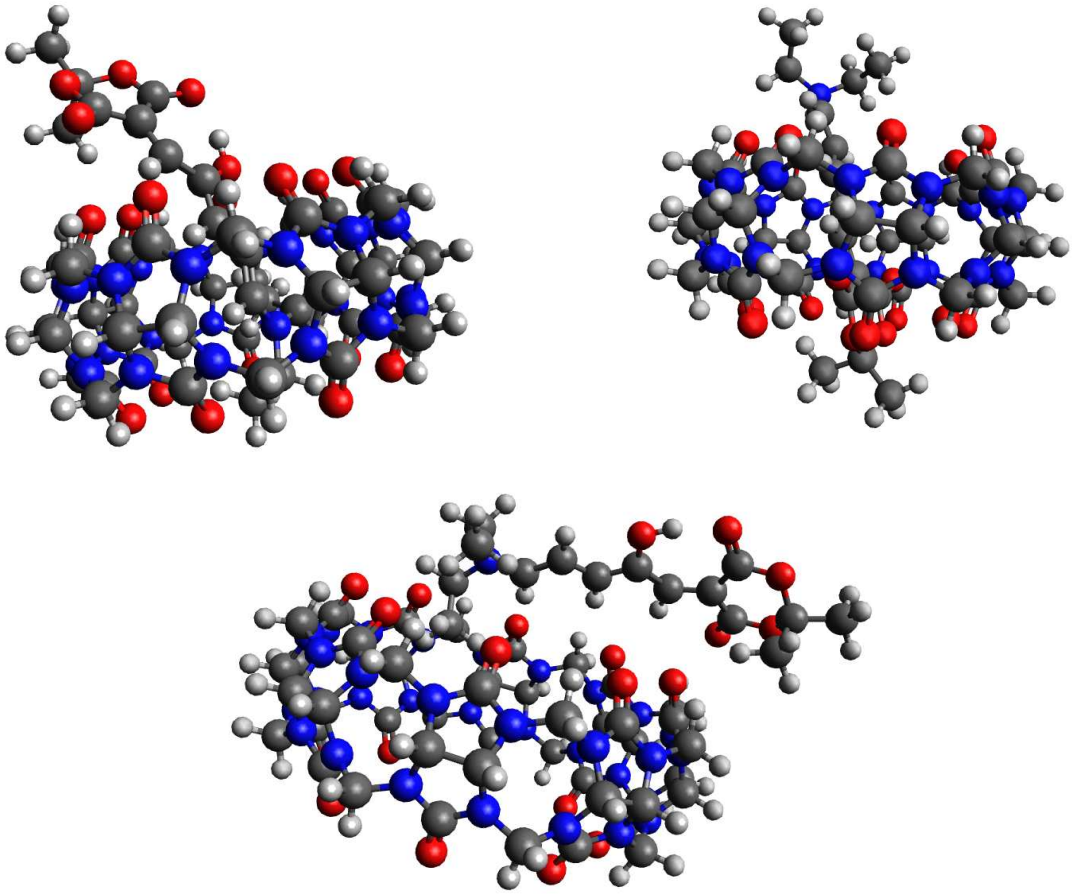

Fig. 36: The simulated complexes of oDASA with CB[7] (top left), protonated oDASA with CB[7] (top right) and oDASA with CB[8]

CONCLUSION

In this work, donor–acceptor Stenhouse adduct (DASA) based on Meldrum's acid was analysed and described by an innovative application of long-existing methods. The result of the whole research can be presented in four parts.

The identification of the form of DASA (whether closed or open) using ESI-IT-MS is probably possible: the data show differences in fragmentation in a protic environment between the samples of supposedly closed and open DASA. The fragmentation also implies, that the pattern is applicable to other DASAs based on Meldrum's acid, since the initial fragmentation occurs on this moiety. However, in order to prove our theory, blind tests need to be executed.

NMR and UV-Vis spectrophotometry were used to analyse the supramolecular behaviour of DASA with CB[7] and CB[8]. From the possible combinations, only open DASA with CB[7] creates an internal complex, in other cases only external interactions are possible. Because of the problems with defining the exact concentration of open DASA in a sample, the binding constant was roughly determined using competitive titrations by different competitors, whose binding constant with CB[7] is already known. The approximate binding constant of the complex oDASA@CB[7] is somewhere between $9.6 \cdot 10^3$ and $4.2 \cdot 10^4$ M^{-1}. [55, 56]

The last part was added to the other experiments as a reaction to the problems caused by the behaviour of DASA in water. Despite the weak results from the experiments on the phase boundary, is it possible to use them for further research. As mentioned at the beginning, the thesis had a potential to open new doors and show the way forward. The perspective is quite vast. In addition to the mentioned research by ESI-MS, many additional supramolecular experiments can be performed: the formation of oDASA@CB[7] is now confirmed in an aqueous neutral environment at room temperature, therefore modifying these conditions and then analysing the results could be interesting.

From the mathematical models, one of the unproven suppositions was that protonated oDASA creates a stronger complex with CB[7] than the neutral one, therefore, experiments affected by variable acidity could bring interesting results (not only) for biological applications, since the acidity of the organism varies between the

different organs and tissues. However, in order to achieve more specific results, the main problem to solve is the poor yield of complexed oDASA and in my opinion that should be the main focus of research before continuing with discovering further biological applications. One of the ideas is to experiment with complexation on the phase boundary but with an assisted transition between the phases instead of a spontaneous diffusion.

LIST OF FIGURES

LIST OF TABLES

REFERENCES

[1] Steed, J. W.; Atwood, J. L. *Supramolecular Chemistry*, 2nd ed.; John Wiley & Sons, Ltd, 2009.

[2] Saraswathi, S. K.; Joseph, J. Thymine-Induced Dynamic Switching of Self-Assembled Nanofibers in Diaminotriazine-Functionalized Tetraphenylethylene Derivatives: Implications for One-Dimensional Molecular Devices. *ACS Appl. Nano Mater.* **2022**, *5*, 3018–3027. DOI: 10.1021/acsanm.2c00310.

[3] Del Regno, R.; et al. Molecular Recognition in an Aqueous Medium Using Water-Soluble Prismarene Hosts. *Org. Lett.* **2022**, *24*, 2711–2715. DOI: 10.1021/acs.orglett.2c00819.

[4] Yoshiko, T.; Sato, D.; Yamamoto, T. Fibrous self-assembly of liquid crystal made by self-organisation. *Liquid Crystals Today* **2022**, *31*, 64–72. DOI: 10.1080/1358314X.2022.2179827.

[5] Freeman, W. A.; Mock, W. L.; Shih, N. Y. Cucurbituril. *J. Am. Chem. Soc.* **1981**, *103*, 7367–7368. DOI: 10.1021/ja00414a070.

[6] Lagona, J.; Mukhopadhyay, P.; Chakrabarti, S.; Isaacs, L. The Cucurbit[*n*]uril Family. *Angew. Chem.* **2005**, *44*, 4844–4870. DOI: 10.1002/anie.200460675.

[7] Escobar, E. C.; Sio, J. E. L.; Torrejos, R. E. C.; Kim, H.; Chung, W.; Nisola, G. M. Organic ligands for the development of adsorbents for Cs+ sequestration: A review. *Journal of Industrial and Engineering Chemistry* **2022**, *107*, 1–19. DOI: 10.1016/j.jiec.2021.11.039.

[8] Barooah, N.; Mohanty, J.; Bhasikuttan, A. C. Cucurbituril-Based Supramolecular Assemblies: Prospective on Drug Delivery, Sensing, Separation, and Catalytic Applications. *Langmuir* **2022**, *38*, 6249–6264. DOI: 10.1021/acs.langmuir.2c00556.

[9] Du, X.; Gu, H.; Liu, X. Selective and reversible chemical sensor for methamphetamine detection using AIEgen and cucurbit[7]uril. *Chin. J. Anal. Chem.* **2022**, *51*, 100275. DOI: 10.1016/j.cjac.2023.100275.

[10] Petkau-Milroy, K.; Brunsveld, L. Supramolecular chemical biology; bioactive synthetic self-assemblies. *Org. Biomol. Chem.* **2013**, *11*, 219–232. DOI: 10.1039/c2ob26790j.

[11] Espanol, E. S.; Villami, M. M. Calixarenes: Generalities and Their Role in Improving the Solubility, Biocompatibility, Stability, Bioavailability, Detection, and Transport of Biomolecules. *Biomolecules* **2019**, *9*, 90. DOI: 10.3390/biom9030090.

[12] Song, N.; Lou, X.; Ma, L.; Gao, H.; Yang, Y. Supramolecular nanotheranostics based on pillarenes. *Theranostic* **2019**, *9*, 3075–3093. DOI: 10.7150/thno.31858.

[13] Havel, V.; Sadilová, T.; Šindelář, V. Unsubstituted Bambusurils: Post-Macrocyclization Modification of Versatile Intermediates. *ACS Omega* **2018**, *3*, 4657–4663. DOI: 10.1021/acsomega.8b00497.

[14] Ullah, F.; Khan, T.; Iltaf, J.; et al. Heterocyclic Crown Ethers with Potential Biological and Pharmacological Properties: From Synthesis to Applications. *Appl. Sci.* **2022**, *12*, 1102. DOI: 10.3390/app12031102.

[15] Tan, S. Y.; Ang, C. Y.; Zhao, Y. Smart Therapeutics Achieved via Host–Guest Assemblies. *Comprehensive Supramolecular Chemistry II*, 2nd ed.; Elsevier, 2017; Chapter 5.17, pp 391–420.

[16] Mutihac, R. C.; Bunaciu, A. A.; Buschmann, H. J.; Mutihac, L. A brief overview on supramolecular analytical chemistry of cucurbit[n]urils and hemicucurbit[n]urils. *J. Incl. Phenom. Macrocycl. Chem.* **2020**, *98*, 137–148. DOI: 10.1007/s10847-020-01019-5.

[17] Barooah, N.; Pemberton, B. C.; Sivaguru, J.; Manipulating Photochemical Reactivity of Coumarins within Cucurbituril Nanocavities. *Organic Letters* **2008**, *10*, 2176–2177. DOI: 10.1021/ol801256r.

[18] Choi, S.; Park, S. H.; Ziganshina, A. Y.; et al. A stable cis-stilbene derivative encapsulated in cucurbit[7]uril. *Chem. Commun.* **2003**, 10027. DOI: 10.1039/b306832c.

[19] Cheung, L. H.; Kajitani, T.; Leung, F. K.; Visible-light controlled supramolecular transformations of donor- acceptor Stenhouse adducts amphiphiles at multiple length-scale. *J. Colloid Interface Sci.* **2022**, *628*, 984–993. DOI: 10.1016/j.jcis.2022.08.034.

[20] Fukuhara, G.; Analytical supramolecular chemistry: Colorimetric and fluorimetric chemosensors. *J. Photochem. Photobiol., C* **2020**, *42*, 100340. DOI: 10.1016/j.jphotochemrev.2020.100340.

[21] Monti, S.; Manet, I. Supramolecular photochemistry of drugs in biomolecular environments. *Chem. Soc. Rev.* **2014**, *43*, 4051–4067. DOI: 10.1039/c3cs60402k.

[22] Dutta Chodhury, S.; Pal, H. Supramolecular and Suprabiomolecular Photochemistry: A Perspective Overview progress and key challenges. *Phys. Chem. Chem. Phys.* **2020**, *22*, 23433–23463. DOI: 10.1039/D0CP03981K.

[23] Méndez-Ardoy, A.; Bassani, D. M. Supramolecular photochemistry: recent progress and key challenges. *Faraday Discuss.* **2015**, *185*, 549–558. DOI: 10.1039/c5fd00146c.

[24] Răileanu, M.; Todan, L.; Voicescu, M.; Ciuculescu, C.; Maganu, M. A way for improving the stability of the essential oils in an environmental friendly formulation. *Mater. Sci. Eng., C* **2013**, *33*, 3281–3288. DOI: 10.1016/j.msec.2013.04.012.

[25] Jullian, C.; Brossard, V.; Gonzalez, I.; Alfaro, M.; Olea-Azar, C. Cyclodextrins-Kaempferol Inclusion Complexes: Spectroscopic and Reactivity Studies. *J. Solution Chem.* **2011**, *40*, 727–739. DOI: 10.1007/s10953-011-9674-6.

[26] Pinho, E.; Grootveld, M.; Soares, G.; Henriques, M. Cyclodextrins as encapsulation agents for plant bioactive compounds. *Carbohydr. Polym.* **2014**, *101*, 121–135. DOI: 10.1016/j.carbpol.2013.08.078.

[27] Kang, B.; Lee, S.; Ng, C.; Kim, J.; Park, J. Exploring the Preparation of Albendazole-Loaded Chitosan-Tripolyphosphate Nanoparticles. *Molecules* **2015**, *8*, 486–498. DOI: 10.3390/ma8020486.

[28] Shanker, G.; Kumar, C. K.; Gonugunta, C.; Kumar, B. V.; Veerareddy, P. R. Formulation and evaluation of bioadhesive buccal drug delivery of tizanidine hydrochloride tabletsSpectroscopic and Reactivity Studies. *Pharm. Sci. Tech.* **2009**, *10*, 530–539. DOI: 10.1208/s12249-009-9241-2.

[29] Lázaro, C. M.; de Oliveira, C.; Gambero, A.; et al. Evaluation of Budesonide–Hydroxypropyl-β-Cyclodextrin Inclusion Complex in Thermoreversible Gels for Ulcerative Colitis. *Dig. Dis. Sci.* **2020**, *65*, 3297–3304. DOI: 10.1007/s10620-020-06075-y.

[30] Qian, Q.; Shi, L.; Gao, X.; et al. A Paclitaxel-Based Mucoadhesive Nanogel with Multivalent Interactions for Cervical Cancer Therapy. *Small* **2019**, *15*, 1903208. DOI: 10.1002/smll.201903208.

[31] Bilensoy, E., Ed. Cyclodextrins in pharmaceutics, cosmetics, and biomedicine: current and future industrial applications, 1st ed.; John Wiley & Sons, Inc.: Hoboken, 2011.

[32] Das, D.; Assaf, K. I.; Nau, W. N. Applications of Cucurbiturils in Medicinal Chemistry and Chemical Biology. *Front. Chem.* **2019**, *7*, 619. DOI: 10.3389/fchem.2019.00619.

[33] Jiao, D.; Geng, J.; Loh, X. J.; Das, D.; Lee, T.; Scherman, O. A. Supramolecular Peptide Amphiphile Vesicles through Host–Guest Complexation. *Angew. Chem.* **2012**, *51*, 9633–9637. DOI: 10.1002/anie.201202947.

[34] Das, S.; Das, T.; Das, P.; Das, D. Controlling the lifetime of cucurbit[8]uril based self-abolishing nanozymes. *Chem. Sci.* **2022**, *13*, 4050–4057. DOI: 10.1039/d1sc07203j.

[35] Zhang, Y.; Yu, Y.; Gao, J. Supramolecular Nanomedicines of *In-situ* Self-Assembling Peptides. *Front. Chem.* **2022**, *10*, 815551. DOI: 10.3389/fchem.2022.815551.

[36] Tam, D. Y.; Ho, J. W.; et al. Penetrating the Blood–Brain Barrier by Self-Assembled 3D DNA Nanocages as Drug Delivery Vehicles for Brain

Cancer Therapy. *ACS Appl. Mater. Interfaces* **2020**, *12*, 28928–28940. DOI: 10.1021/acsami.0c02957.

[37] Klán, P. Organická fotochemie, 1st ed.; Masarykova univerzita v Brně: Brno, 2001.

[38] Persico, M.; Granucci, G. Photochemistry: A Modern Theoretical Perspective, 1st ed.; Springer: Cham, 2018.

[39] Klán, P.; Wirz, J. Photochemistry of Organic Compounds, 1st ed.; John Wiley & Sons, Ltd: Chichester, 2009.

[40] Klessinger, M., Michl, J., Eds. Excited States and Photochemistry of Organic Molecules, 1st ed.; VCH Publishers, Inc.: New York, 1995.

[41] Stenhouse, J. Ueber die Oele, die bei der Einwirkung der Schwefelsäure auf verschiedene Vegetabilien entstehen. *Justus Liebigs Ann. Chem.* **1850**, *74*, 278–297.

[42] Helmy, S.; Oh, S.; Leibfarth, F. A.; Hawker, C. J.; Read de Alaniz, J. Design and Synthesis of Donor-Acceptor Stenhouse Adducts: A Visible Light Photoswitch Derived from Furfural. *J. Org. Chem.* **2014**, *79*, 11316–11329. DOI: 10.1021/jo502206g.

[43] Stenhouse, J. Ueber Furfuranilin und Furfurtoluidin. *Justus Liebigs Ann. Chem.* **1870**, *156*, 195–205.

[44] Schiff, H. Ueber Farbstoffbasen aus Furfurol. *Justus Liebigs Ann. Chem.* **1887**, *239*, 349–385.

[45] Honda, K.; Komizu, H.; Kawasaki, M. Reverse Photochromism of Stenhouse Salts. *J. Chem. Soc., Chem. Commun.* **1982**, 253–254. DOI: 10.1039/C39820000253.

[46] D'Arcy, B. R.; Lewis, K. G.; Mulquiney, C. E. Reaction of Stenhouse salts. III. Transformation Products Under Acidic and Basic Conditions. *Aust. J. Chem.* **1985**, *38*, 953–965. DOI: 10.1071/CH9850953.Odc

[47] Huang, Y.; Du, Y.; Yuan, L.; Chu, Z.; He, L. Donor-acceptor Stenhouse adducts as new emerging photoswitches: synthesis, light-responsive properties, and

applications in polymer science. *J. Macromol. Sci., Pure Appl. Chem.* **2021**, *58*, 717–724. DOI: 10.1080/10601325.2021.1936550.

[48] Lerch, M. M.; Szymański, W.; Feringa, B. L.The (photo)chemistry of Stenhouse potoswitches: guiding principles and system design. *Chem. Soc. Rev.* **2018**, *47*, 1910–1937. DOI: 10.1039/c7cs00772h.

[49] Wang, D.; Zhao, L.; Zhao, H.; et al. Inducing molecular isomerization assisted by water. *Communications Chemistry* **2019**, *2*, 118. DOI: 10.1038/s42004-019-0221-5.

[50] Payne, L.; Josephson, J. D.; Murphy, R. S.; Wagner, B. D. Photophysical Properties of Donor-Acceptor Stenhouse Adducts and Their Inclusion Complexes with Cyclodextrines and Cucurbit[7]uril. *Molecules* **2020**, *25*, 4928. DOI: 10.3390/molecules25214928.

[51] Hemmer, J. R.; Page, Z. A.; Clark, K.; Stricker, F.; Dolinsky, N. D.; Hawker, C.; Read de Alaniz, J. Controlling Dark Equilibria and Enhancing DASA Photoswitching Properties Through Carbon Acid Design. *J. Am. Chem. Soc.* **2018**, *140*, 10425–10429. DOI: 10.1021/jacs.8b06067.

[52] Sroda, M. M.; Stricker, F.; Peterson, J. A.; Bernal, A.; Read de Alaniz, J. Donor–Acceptor Stenhouse Adducts: Exploring the Effects of Ionic Character. *Chem. Eur. J.* **2021**, *27*, 4183–4190. DOI: 10.1002/chem.202005110.

[53] Lerch, M.; Medveď, M.; Lapini, A.; et al. Tailoring Photoisomerization Pathways in Donor-Acceptor Stenhouse Adducts: The Role of the Hydroxy Group. *J. Chem. Phys.* **2018**, *122*, 955–964. DOI: 10.1021/acs.jpca.7b10255.

[54] Alnajjar, M. A. Cucurbituril Complexes and their Spectral Characterization. PhD. Dissertation, Jacobs University Bremen, 29/07/2021.

[55] Wyman, I. W.; Macartney, D. H. Cucurbit[7]uril host–guest complexes with small polar organic guests in aqueous solution. *Org. Biomol. Chem.* **2008**, *6*, 1796–1801. DOI: 10.1039/b801650j.

[56] Liu, S.; Ruspic, C.; Mukhopadhyay, P.; Chakrabarti, S.; Zavalij, P.; Isaacs, L. The Cucurbit[*n*]uril Family: Prime Components for Self-Sorting Systems. *J. Am. Chem. Soc.* **2005**, *127*, 15959–15967. DOI: doi.org/10.1021/ja055013x.

[57] Berraud-Pache, R.; Santamaria-Aranda, E.; de Souza, B.; Bistoni, G.; Neese, F.; Sampedro, D.; Izsák, R. Redesigning donor-acceptor Stenhouse adduct photoswitches through a joint experimental and computional study. *Chem. Sci.* **2021**, *12*, 2916–2924. DOI: 10.1039/d0sc06575g.